NASA Contractor Report 3153

Electron Spectroscopy for Chemical Analysis (ESCA) Study of Atmospheric Particles

John G. Dillard, Roland D. Seals,
and James P. Wightman

CONTRACT NAS1-13175-2
JUNE 1979

NASA

NASA Contractor Report 3153

Electron Spectroscopy for Chemical Analysis (ESCA) Study of Atmospheric Particles

John G. Dillard, Roland D. Seals,
and James P. Wightman
Virginia Polytechnic Institute and State University
Blacksburg, Virginia

Prepared for
Langley Research Center
under Contract NAS1-13175-2

National Aeronautics
and Space Administration

**Scientific and Technical
Information Branch**

1979

TABLE OF CONTENTS

LIST OF TABLES

LIST OF FIGURES

GLOSSARY

EDAX - Energy Dispersive Analysis of X-rays

ESCA - Electron Spectroscopy for Chemical Analysis

NAA - Neutron Activation Analysis

PWHM - Peak Width at Half Maximum

SEM - Scanning Electron Microscopy

XPS - X-ray Photoelectron Spectroscopy

Identification of commercial products in this report is to adequately describe the materials and does not constitute official endorsement, expressed or implied, of such products or manufacturers by the National Aeronautics and Space Administration.

I. SUMMARY

The ESCA (Electron Spectroscopy for Chemical Analysis) analysis of atmospheric particles collected on Nuclepore filters is presented. Samples were collected on gold coated and on uncoated filters. Collection of the particles on the filters was performed by NASA personnel from the Langley Research Center. Samples were taken at Norfolk, Virginia and also at the NASA-Kennedy Space Center (KSC). It was demonstrated that with the ESCA technique, it was possible to identify the chemical (bonding) state of elements contained in the atmospheric particulate matter collected on Nuclepore filters. Standardization procedures have been developed for measuring the absolute binding energies using the silicon contained in the filter paper as a calibration element. Sulfur, nitrogen, mercury, chlorine, alkali, and alkaline earth metal species were identified in the Norfolk samples. Assignment of the chemical state of each element was accomplished by comparing measured binding energies for authentic materials with the test samples. ESCA binding energy data for aluminum indicated that three chemically different types of aluminum are present in the launch and background samples from NASA-KSC.

In addition to ESCA measurements, neutron activation analysis (NAA) was performed on all samples. Scanning electron microscopy (SEM) was used to determine particle shape and distribution. Energy dispersive analysis of X-rays (EDAX) was done simultaneously with SEM to corroborate the NAA results. SEM photomicrographs revealed that the particles collected at NASA-KSC during launch have unique spherical shapes when compared with the particles collected during launch inactivity and at the Norfolk sampling site.

Particulate matter identification and characterization can be carried out in a definitive manner using ESCA. NAA and SEM/EDAX have severe limitations in detecting certain key elements, namely carbon, nitrogen, oxygen and sulfur. Further, it is impossible with either NAA and/or SEM/EDAX to determine the chemical state in which each element is found. It is clear from this study that the ESCA technique is uniquely suited to establish the chemical state of elements contained in airborne particulate matter which has been collected on filter paper.

II. INTRODUCTION

A. Objectives

The present work is divided into two parts, namely, the ESCA analysis of particles collected at Norfolk, Virginia and the ESCA analysis of particles collected at the NASA-Kennedy Space Center (KSC).

The objectives of the first phase of the work were to:

1. perform ESCA analysis on particles collected on gold coated and uncoated Nuclepore filters at Norfolk;
2. measure ESCA spectra for a number of authentic materials; and
3. examine the particulate matter collected on the Nuclepore filters by scanning electron microscopy.

The objectives of the second phase of the work were to:

1. perform ESCA analysis for aluminum on particulate matter collected at ground stations, by aircraft flights through the exhaust cloud, and on ocean vessel sampling stations at the NASA-KSC during rocket launch activity and inactivity periods;
2. measure ESCA spectra for aluminum in authentic aluminum-containing materials; and,
3. examine the particulate matter collected on the Nuclepore filters by scanning electron microscopy to aid in identifying the collected particulate matter.

It should be noted that the results of the characterization by other analysis methods of both the Norfolk samples (1) and NASA-KSC samples (2) have been published.

B. Literature

The need for the chemical analysis of atmospheric particles has been cited in recent summaries concerned with the impact of man on his environment (3-5). There have been several techniques reported for the analysis of atmospheric particles including neutron activation analysis, X-ray

fluorescence, proton scattering and X-ray analysis in conjunction with scanning electron microscopy. Harris (6) has published an excellent literature summary of atmospheric aerosols. The physical characteristics and chemical composition of such aerosols including analysis techniques are presented. However, many of the techniques which are used currently are limited in the sense that although element identity may be established, the actual chemical (bonding) state is not.

The recent development of electron spectroscopy for chemical analysis (ESCA) appears to be a powerful analytical technique for the chemical identification of atmospheric particles collected on filters (7). Various ESCA studies of metal and non-metal species have demonstrated (8-24) the usefulness of this method in distinguishing between different chemical states of various elements. ESCA studies have been carried out with the goal of identifying the chemical state of sulfur (9-11,13), nitrogen (9, 11-15), silicon (16-19), aluminum (18-20), iron (21,22) lead (11,13) and zinc (23) in minerals and in particulate matter related to atmospheric pollution. In the studies of sulfur compounds and particularly those of samples collected (Lundgren cascade impactor) in a metropolitan atmospheric environment (9,10), the ESCA results permit identification of the sulfur as sulfate, sulfur dioxide, or sulfide. The identification was accomplished by comparing the sample binding energies with those of known compounds (8-11, 24). Examination of the ESCA spectra of various aluminum-containing materials has revealed (18-20) subtle differences in the measured binding energies. These differences in core binding energies have been related to structural changes in the aluminum compounds (18-20). These

differences in binding energy suggest that the chemical state of aluminum in particulate matter could be identified using ESCA.

III. EXPERIMENTAL

A. Sample Identification

The samples collected at Norfolk, Virginia were supplied by personnel at the NASA-Langley Research Center (LaRC) and were coded as shown in Table I. The NASA samples were collected on Nuclepore filters using an aerosol membrane holder. Samples coded NASA 1, F-2, 4, and F-12 were collected on gold-coated Nuclepore filters and NASA 13 was collected on uncoated Nuclepore filters. NASA 38A and 74A were blank gold-coated and blank uncoated Nuclepore filters, respectively.

Samples were obtained at NASA-Kennedy Space Center (KSC) for 24 hours during launch inactivity and for shorter periods during launch activities of solid propellant boosters. The 24 hour background samples were obtained to provide base-line data on the aluminum level and chemical identity during inactivity. Samples collected during launch were obtained at ground stations, by aircraft flights through the exhaust cloud, and on an ocean vessel stationed under the exhaust cloud. Samples collected at NASA-KSC were supplied by personnel at the NASA-LaRC and were designated as shown in Table I.

B. Neutron Activation Analysis (NAA)

Neutron activation analyses (NAA) were obtained using the facilities of the VPI and SU Nuclear Research Laboratory and the results provided by personnel at the NASA-LaRC.

TABLE I

SAMPLE IDENTIFICATION

NORFOLK, VIRGINIA SAMPLES

Designation		Collection Date	Collection Time
SAMPLES	NASA 1	8-11-73	0700-0900
	NASA F-2	8-13-14-73	1800-0600
	NASA 4	8-13-73	0900-1800
	NASA F-12	8-14-73	0600-1200
	NASA 13	---	---
BLANKS	NASA 38A	---	---
	NASA 74A	---	---

NASA-KSC SAMPLES

Type	Designation	Filter Side Containing Particles
Ocean	75-A-20 (P-4)	Dull
Ocean	75-A-21 (P-2)	Shiny
Aircraft	75-A-41 (A-1)	Dull
Aircraft	75-A-47 (A-7)	Dull
Ground	75-A-161 (S204)	Dull
Ground	75-A-174 (P4)	Dull
Background	75-A-179	Shiny
Background	75-A-181	Shiny

C. Scanning Electron Microscopy (SEM)

The distribution, size, and shape of the particulate matter on each sample were obtained using an AMR (Advanced Metals Research) Model 600 scanning electron microscope. Photomicrographs were made of the particles at magnifications ranging from X100 to X10,000. Energy dispersive analysis of X-rays (EDAX) measurements on several particles in each sample were made to identify certain elements. The 5 x 5 mm samples of the SEM studies were mounted on aluminum stands using copper tape and vapor-deposited with a gold-palladium alloy to minimize charging.

D. Electron Spectroscopy for Chemical Analysis (ESCA)

Photoelectron spectra were measured with an A.E.I. ES100 photoelectron spectrometer using aluminum $K\alpha_{1,2}$ X-radiation (1486.6 eV). The core electron binding energies were obtained on a 4 x 10 mm sample mounted on a copper probe by Scotch double stick tape. The Si $2p_{1/2,3/2}$ and Si $2s_{1/2}$ levels were measured and used to evaluate the spectrometer work function and the extent of charging during each sample measurement. Accurate binding energies for the silicon levels were determined in a series of experiments by measuring the binding energy for each silicon level relative to the more accurately known gold $4f_{5/2}$ and $4f_{7/2}$ levels at 87.1 and 83.4 eV, respectively (25). The measured binding energies (BE) for the silicon levels were BE $(2p_{1/2,\ 3/2})$ = 101.7 ± 0.1 eV and BE $(2s_{1/2})$ = 152.5 ± 0.1 eV.

The data were collected by a Digital PDP 8/e computer on paper tapes for subsequent processing in a Digital PDP 8/I computer using the MADCAP IV program for plotting spectra. Deconvolutions were performed using the GASCAP IV program (26).

Typical scan times for the Norfolk samples were 24 hours for three elements due to the low particle concentrations. THe aluminum concentration on the NASA-KSC filters was so low it was necessary to scan the core level binding energy regions of interest for about 20-35 hours. Only after scanning for this time period could adequate counts on the aluminum 2p core levels be obtained.

E. Standards

To elucidate the chemical state of the particles collected at Norfolk, the standard samples listed in Table II were collected on Nuclepore membrane filters. All chemicals were reagent grade, purchased from commercial sources - J. T. Baker Chemical Co. or Fisher Scientific Company - and were used without additional purification. The chemicals were ground using a Spec Mill - a mechanical grinder using a metal container and balls made of tungsten carbide. The size of the particles after 30 minutes of grinding was estimated to be 45 to 75 μm using a 325 mesh to 160 mesh sieve. The particles for Na_2SO_3/74A and Na_2SO_4/74A were not ground. Particle collection was carried out in a reaction chamber of glass (3000 ml volume) that housed the aerosol membrane holder and an air inlet glass hose to blow the particles.

All standard samples were collected on blank, uncoated Nuclepore filters, NASA 74A. The particles on each sample were collected for four 30-minute intervals. In between each interval, the membrane holder was shaken to remove loose particles. This procedure was used to collect Dusts B-3, B-4, B-5, B-6, Na_2SO_3, and Na_2SO_4. Dusts B-4, B-5, and B-6 contained the compounds in a 1:1 ratio by weight of sulfur.

TABLE II

STANDARD IDENTIFICATION

Name	Composition
Dust B-2	Al_2O_3, ZnS, Na_2CO_3, $FeSO_4$, S
Dust B-3	S
Dust B-4	ZnS, $FeSO_4$
Dust B-5	ZnS, Na_2SO_3
Dust B-6	HgS, Na_2SO_4
SO_2/74A	SO_2, gas
NH_3/74A	NH_3, gas
Na_2SO_4/74A	Na_2SO_4
Na_2SO_3/74A	Na_2SO_3
Hg/NASA 74A-1	Hg
Hg/NASA 74A-2	Hg
Hg/NASA 38A	Hg

Since mercury was detected on some of the samples by ESCA, standard mercury-containing filters were prepared. Samples designated Hg/NASA 38A, and Hg/NASA 74A were made by slightly heating elemental mercury and collecting the vapors on Nuclepore filters using the collection chamber.

Samples designated SO_2/NASA 74A and NH_3/NASA 74A were made by passing gaseous SO_2 or NH_3 into the collection chamber. Each gas was passed over water and was collected for 15 minutes on NASA 74A Nuclepore filters. For the SO_2 and NH_3 experiments, the pH of the water and the air passing through the pump was 2-3 and 10-11 respectively.

The primary emphasis on the particles collected at the NASA-KSC was the analysis of aluminum. To obtain a group of reference aluminum core binding energies, a number of standard aluminum samples were dusted onto uncoated Nuclepore filters in the manner described above and the Al 2p binding energies were measured. The standard samples were all reagent grade materials and were used without additional purification. The samples designated Al_2O_3.X(X=HCl and CO) were prepared from the corresponding α- or γ-Al_2O_3 by heating alumina in vacuo for two hours at 80°C, followed by holding at 40°C for two hours, and then exposure of the alumina to the test gas (HCl or CO) at about 20 torr for several hours. Samples were then collected on Nuclepore filters for ESCA measurements. The standard samples were selected to characterize aluminum in different chemical (bonding) states. The samples included aluminum in electron deficient environments, Na_3AlF_6 and $AlCl_3$ as well as samples where aluminum is found in a richer electron environment, i.e., the $Al_2O_3.nH_2O$ samples.

IV. RESULTS AND DISCUSSION

PART I. NORFOLK, VIRGINIA SAMPLES

A. Neutron Activation Analysis (NAA)

The neutron activation analysis (NAA) results expressed in ppm are summarized in Table III for NASA samples. Primarily, only those elements whose concentrations exceeded 300 ppm in any sample are included in Table III. Note that the same entries are made for Al and for Si in Table III. The NAA results are ambiguous as regards the analysis of Al and Si. The reasons for this ambiguity are the small sample submitted ($\sim$ 1500 μg) and the use of mixed thermal and fast neutron activation. Thus, in the Fall of 1974 when the NAA was performed, it was not possible to differentiate between Al and Si.

B. Scanning Electron Microscopy (SEM)

The SEM photomicrographs were obtained at various magnifications for all samples. A SEM photomicrograph (2000X) of a gold-coated blank Nuclepore filter (NASA 38A) is shown in Figure 1. The uniformity of pore size is apparent and the gold coating does not cover the pores. A low magnification (500X) photomicrograph of NASA 1 is shown in Figure 2. A variety of particle shapes and sizes are seen.

A low magnification (100X) photomicrograph of NASA F-2 is shown in Figure 3. Here the strips characteristic of the sample collector are seen. A higher magnification photomicrograph of this sample is seen in Figure 4 (10,000X). The holes in the Nuclepore filters are clearly seen. It is significant that the filter surface is not completely covered with particles. In fact, less than 50% of the surface is covered as gauged subjectively by Figure 4. The less than complete coverage

TABLE III

SUMMARY OF NAA RESULTS FOR NASA-NORFOLK SAMPLES

Element	Sample				
	1	F-2	4	F-12	13
Al, Si	360*	1584	2442	2504	972
Ca	313	1821	2630	2040	3570
Cd	188	377	29	78	47
Cl	106	142	126	105	3650
Fe	---	---	---	---	---
Hg	101?	76?	350?	---	0.4
K	2000	7300?	9600?	380	390
Mg	110	270	500	630	870
Na	410	430	470	1190	4200
Ti	170	128	440	313	54
Zn	25	90	65	135	62

*Concentrations expressed in ppm.

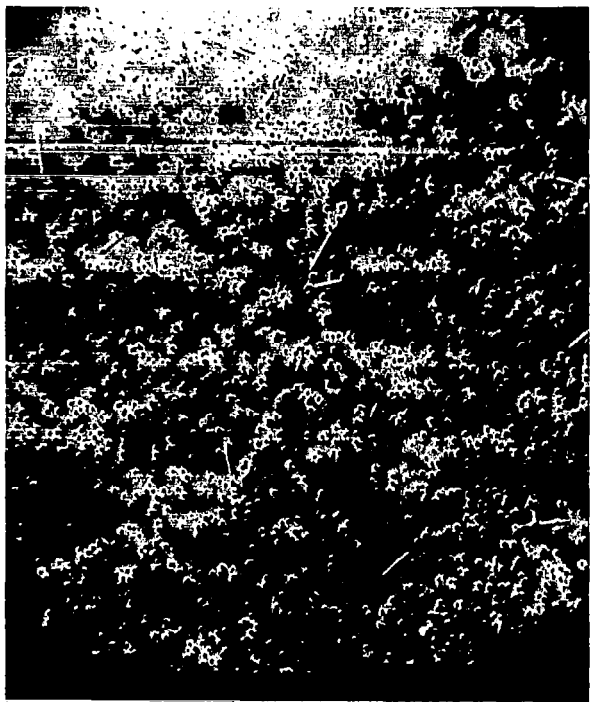

Fig. 1. SEM Photomicrograph (2000X) - NASA 33A, gold coated Nucleopore filter

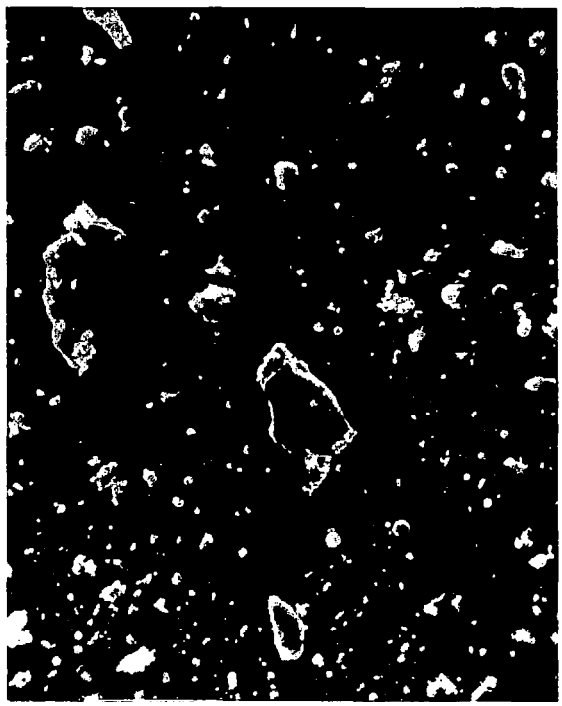

Fig. 2. SEM Photomicrograph (500X) - NASA 1

Fig. 3. SEM Photomicrograph (100X) - NASA F-2

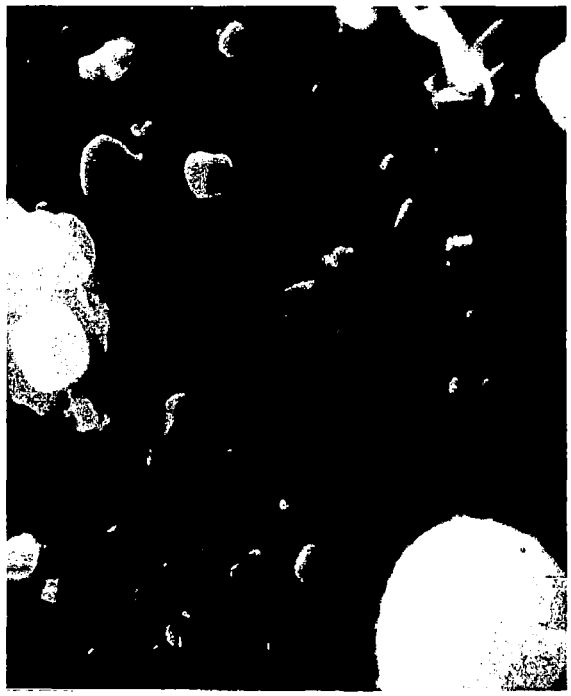

Fig. 4. SEM Photomicrograph (10,000X) - NASA F-2

accounted for the long times for the ESCA analysis of samples as noted in the Experimental Section.

A low magnification (500X) photomicrograph of NASA 4 is shown in Figure 5. Again, a heterogeneous collection of particles is seen. The same observation is noted in NASA F-12 where the photomicrograph at 500X is shown in Figure 6. The larger particles in Figure 6 range from 12 to 16 μm.

A photomicrograph at 500X is shown in Figure 7 for NASA 13. Ca and Cl were detected by EDAX of the "arrowhead" particle (lower right in Figure 7) whereas Si and S were detected by EDAX of the elongated particle at top of the "arrowhead" (Figure 7). The ESCA spectra shows the absence of Ca but strong Cl, Si, and S signals. High Ca and Cl concentrations were noted in the NAA results. This is a fairly typical comparison of the results of the SEM/EDAX, ESCA, and NAA. However, the results are not necessarily contradictory since NAA and SEM/EDAX are bulk techniques where ESCA is a surface technique. Another point to note is that the assignment of elemental analysis based on EDAX is often ambiguous due to the overlap of characteristic peaks of several elements.

A photomicrograph (500X) of a laboratory collected sample B-2 is seen in Figure 8. The particles are rather randomly dispersed on the Nuclepore filter and are not as heterogeneous as in the NASA samples.

C. ESCA Analysis

1. Introduction

Analysis using ESCA is particularly unique in that only data from the surface (2.5-5.0 nm) of the sample is obtained. The principle of ESCA or X-ray photoelectron spectroscopy (XPS) is based on measuring the

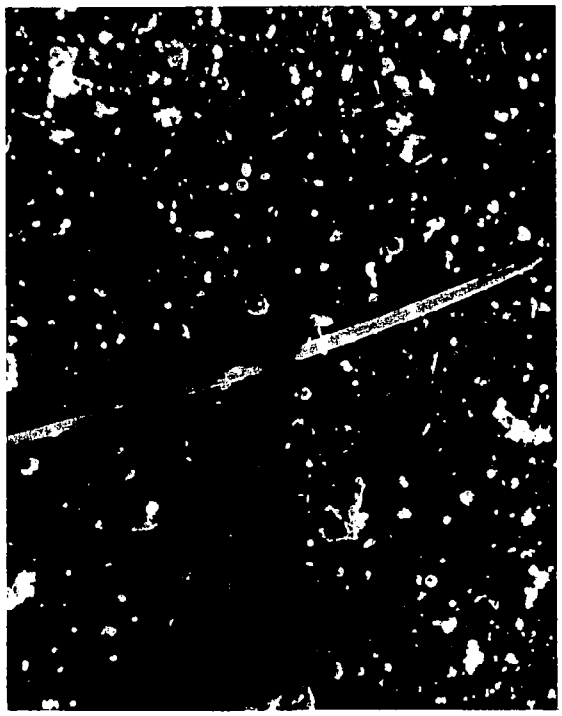

Fig. 5. SEM Photomicrograph (500X) - NASA 4

Fig. 6. SEM Photomicrograph (500X) - NASA F-12

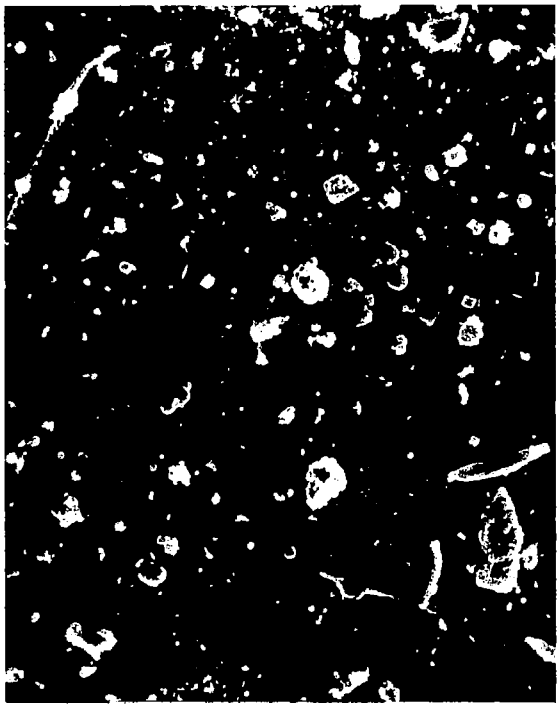

Fig. 7. SEM Photomicrograph (500X) - NASA 13

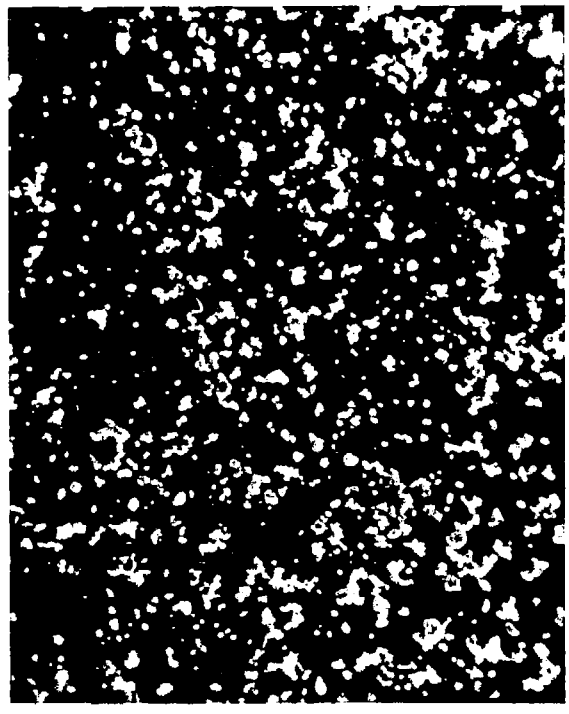

Fig. 8. SEM Photomicrograph (500X) - Dust B-2

kinetic energy of electrons ejected from a sample upon bombardment of the sample by X-rays. From this experimental measurement the binding energy of the electron can be evaluated from the following expression:

$$h\nu = BE + KE + \phi$$

where $h\nu$ is the energy of the soft X-ray beam

BE is the binding energy of the electronic state of a given element

KE is the kinetic energy of the photoejected electron

ϕ is the work function - an instrumental correction factor used to calibrate the energy scale

In the studies reported here $h\nu$ is fixed at 1486.6 eV by using an aluminum X-ray target. The work function is measured in each experimental determination by referencing all values to an internal standard in the samples, silicon. Kinetic energy is measured by varying the potential between two hemispherical plates of an electrostatic analyzer.

ESCA data were collected on (i) gold coated and uncoated blank Nuclepore filters, (ii) several gold coated and uncoated Nuclepore filters on which authentic well characterized compounds had been deposited, and (iii) 5 NASA samples. Measurements on blank filters were carried out to determine which elements characteristic of the paper could complicate analysis of the particles. Determination of the binding energies for authentic samples was necessary to confirm the chemical identity of the species detected on NASA test samples.

Because absolute binding energies were needed to identify the elements present and to establish the chemical nature of the species present on the Nuclepore filters, the initial phase of the study was concerned

with identifying the major components in gold coated and uncoated filters. In another phase of the work, absolute binding energies of standard samples of materials collected on coated and uncoated filters were measured. Sample materials for this phase were selected from data obtained from scans and absolute binding energy measurements on NASA samples. These "standard" samples were prepared at VPI&SU using gold coated and uncoated Nuclepore filters supplied by NASA. The primary phase of the work centered on measuring the binding energies and identifying the principal constituents of NASA samples on Nuclepore filters. No attempt was made in this study to obtain a quantitative analysis of the NASA samples by ESCA. In the NASA samples, constituents containing nitrogen, sulfur, mercury, calcium, chlorine, sodium, and silicon were detected. A variety of nitrogen- and sulfur-containing materials were noted. The silicon species noted is a prominent elemental constituent in the blank paper. A complete summary of the ESCA data for all NASA samples and the identity for each species are presented in Table IV. Binding energies for NASA samples re-run after some three months storage at VPI&SU are collected in Table V. These stored samples are referred to below as 'aged' NASA samples. As noted above, the identity was established by comparison of measured binding energies in the papers with those of authentic samples collected on blank papers.

The ESCA results discussed here are divided into the following three main areas:

Section 2: The elemental composition of blank and gold coated Nuclepore filters:

TABLE IV

SUMMARY OF ESCA RESULTS FOR NASA-NORFOLK SAMPLES

NASA SAMPLE		1		F-2		4		F-12		13	
	Level	BE(eV)	Species	BE(eV)	Species	BE(eV)	Species	BE(eV)	Species	BE(eV)	Species
Si	$2p_{1/2,3/2}$	101.5	Silicone, paper	101.6	Silicone paper	101.5	Silicone, paper	101.7	Silicone, paper	101.6	Silicone, paper
Si	$2s_{1/2}$	152.3	Silicone, paper	152.4	Silicone, paper	152.6	Silicone, paper	152.7	Silicone, paper	152.8	Silicone, paper
S	$2p_{1/2,3/2}$	ND**		167.9	$SO_2.XH_2O$	168.2*	$S_2O_3^{2-}$?	167.8	$SO_2.XH_2O$	169.3	SO_4^{2-}
							SO_X ?				
N	$1s_{1/2}$	ND		400.8	NO_X,amide	400.1	NO_X,amide	400.8	NO_X,amide	399.7	NH_3,amine
				399.2	NH_3,amine	399.7	NH_3,amine	399.3	NH_3,amine	398.4	CN^-,RCN
Ca	$2p_{1/2,3/2}$	352.8	Ca^{2+}	352.8	Ca^{2+}	352.7	Ca^{2+}	352.7	Ca^{2+}	ND	
Al	$2s_{1/2}$	ND						ND			
Al	$2p_{1/2,3/2}$							ND			
Cl	$2p_{1/2,3/2}$	ND								198.9	Cl^-
Pb	$4f_{5/2,7/2}$					ND		ND			
Na	$2p_{1/2,3/2}$			ND		ND		ND		31.0	Na^+
Na	$2s_{1/2}$			ND		ND					
Mg	$2p_{1/2,3/2}$					ND		ND		ND	
Hg	$4f_{5/2}$	ND[103.5 Hg^o]		ND[102.1 Hg^o]		102.9 Hg^o				ND	
Hg	$4f_{7/2}$	ND[99.7 Hg^o]		ND[99.5 Hg^o]		99.2 Hg^o				ND	
Cd	$3d_{3/2,5/2}$	ND		ND		ND		ND		ND	

*Unidentified Sulfur **ND-Not Detected [] Bracketed values refer to aged samples

TABLE V

BINDING ENERGIES[a] OF AGED NASA-NORFOLK SAMPLES

Sample	Si $2p_{1/2,3/2}$ [b]	Hg $4f_{5/2}$ [c]	Hg $4f_{7/2}$ [c]
NASA 74A	101.7	-----	-----
NASA 38A	101.8	103.3	99.4
NASA F-12	101.2	103.5	99.7
NASA 4	101.5	103.4	99.6
NASA F-2	101.4	103.4	99.5
NASA 1	-----	103.5	99.7
NASA 13	101.6	-----	-----

(a) Binding energies (in eV) are not as precise as data on fresh samples due to distortions caused by Si 2p and Hg 4f overlapping.

(b) Silicon in filter.

(c) Hg (elemental mercury amalgamated with gold on paper). (See Discussion)

Section 3: Binding energy results for standard compounds; and,

Section 4: Elemental analysis and chemical identity of particulates on NASA samples.

2. Elemental composition of blank and gold coated Nuclepore filters

ESCA measurements on blank filters were carried out to determine background elements which might interfere with the identification of atmospheric particles. A survey of constituent elements in the blank paper also was desirous to see whether any element detected in significant abundance could serve as an internal standard for absolute energy calibrations. It was also important to determine whether it was necessary to collect samples on gold coated filter papers or whether collection and identification of particulate matter could be accomplished using uncoated Nuclepore papers.

In the ESCA spectra of uncoated Nuclepore filters (NASA 74A), silicon and iron are the dominant elements. No other species were detected in significant abundance. The measured binding energies for selected Si and Fe energy levels are presented in Table VI and a typical Si $2p_{1/2,3/2}$ spectrum is shown in Figure 9. The binding energies were calibrated using background carbon from the spectrometer whose $1s_{1/2}$ binding energy is 284.3 $\pm$ 0.1 eV. The binding energy for silicon is somewhat lower than that found in aluminosilicates. This would suggest that the silicon in the filter is probably more covalent (silicones) in nature than silicon in silicates. The iron found in the filters is characteristic of iron in the +2 oxidation state. The amount of iron in the filters is significantly less than that of silicon. Scans were made for the following

TABLE VI

BINDING ENERGIES OF SPECIES IN BLANK

NUCLEPORE FILTERS

Species	BE (eV ± 0.1)	level	Calibrant	BE (ev ± 0.1)	level
Uncoated Filter					
Si	101.7	$2p_{1/2,3/2}$*	C (Bkgnd)	284.3	$1s_{1/2}$
Si	152.5	$2s_{1/2}$	C (Bkgnd)	284.3	$1s_{1/2}$
Fe	709.8	$2p_{3/2}$	C (Bkgnd)	284.3	$1s_{1/2}$
Gold Coated Filter					
Si	101.7	$2p_{1/2,3/2}$*	Au	83.4	$4f_{7/2}$
Si	152.5	$2s_{1/2}$	Au	83.4	$4f_{7/2}$

Known Si and Fe Binding Energies

Silicates	BE's = 102.0 - 102.7 eV	$2p_{1/2,3/2}$
Fe^{2+} (salts)	BE's = 710.0 - 710.5 eV	$2p_{3/2}$
Fe^{3+} (salts)	BE's = 712.6 - 713.0 eV	$2p_{3/2}$

* The Si $2p_{1/2,3/2}$ multiplet is not resolved.

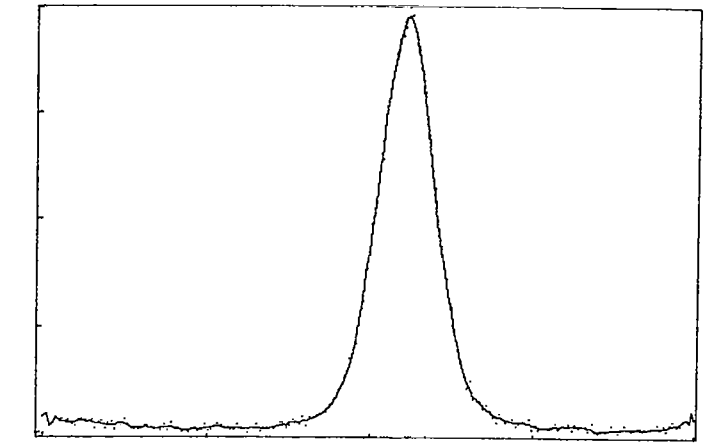

Fig. 9. Si 2p Photopeak - NASA 74A

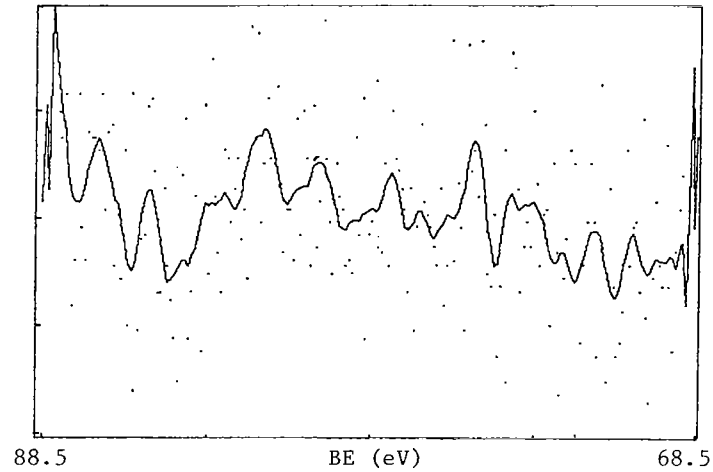

Fig. 10. Al 2p Photopeak - NASA 74A

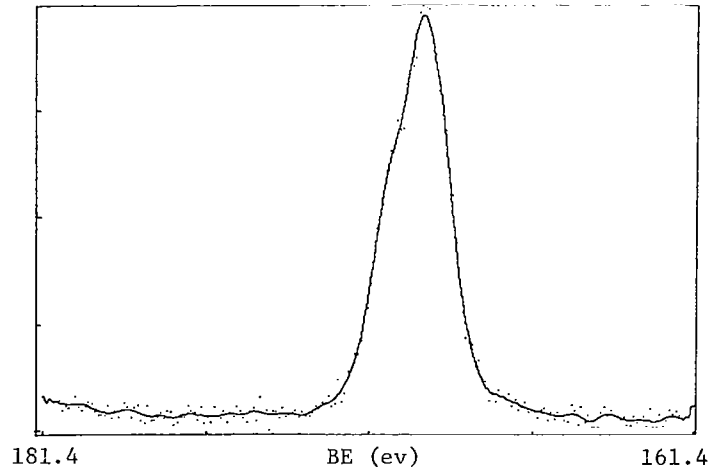

Fig. 11. S 2p Photopeak Na_2SO_4/74A

elements: S, Na, Al, Ca, Mg, and Zn. No detectable signal for any of these elements was obtained as seen in the representative spectrum for Al in Figure 10.

The ESCA measurements on the gold coated Nuclepore filters (NASA 38A) revealed silicon in addition to gold. Since the binding energy for gold is well established (25), the gold values were used to calibrate the silicon $2p_{1/2,3/2}$ and $2s_{1/2}$ energy levels. These values are also summarized in Table VI. Upon examining the data it is clear that the Si $2p_{1/2,3/2}$ and $2s_{1/2}$ levels are reproducible to within the experimental precision of the instrument $\pm$ 0.1 eV. These results also show that either of the Si levels could serve as an internal standard for measuring absolute binding energies. In this investigation both Si levels were used for calibration when uncoated papers were used. When using gold coated papers the gold $4f_{5/2}$ and $4f_{7/2}$ levels and the silicon $2p_{1/2,3/2}$ and $2s_{1/2}$ levels were used.

3. Binding energy results for standard compounds

Since species detected on standard NASA samples were found (see section 4 below) to contain among other elements sulfur, nitrogen, and mercury, it was necessary to determine the binding energies of standard samples collected on uncoated Nuclepore filters. The sulfur-, nitrogen-, and mercury-containing samples investigated are presented in Table VII.

a. Sulfur

The measured binding energies for sulfur from sulfides to sulfates occur in the range from 162.6 eV (S^{2-}) to 169.7 eV (SO_4^{2-}). Binding energies between these limiting values are noted for sulfur as S^{2-} (ZnS)

TABLE VII

IDENTITY AND BINDING ENERGIES OF STANDARD

COMPOUNDS COLLECTED ON UNCOATED NUCLEPORE FILTERS

(CALIBRANT Si ($2p_{1/2,3/2}$), 101.7 eV)

SULFUR

Sample	BE (eV); (±0.1); level $2p_{1/2,3/2}$	Literature
ZnS	163.4	162.2 (10)
CdS	162.6	
HgS	162.6	
S_8	164.1	
Na_2SO_3	166.6	167.0 (10)
Na_2SO_3	168.2	
SO_2	167.5	167.9 (10)
SO_2*	168.3	
SO_2*	163.4	
Na_2SO_4	169.7	169.0 (10)
$FeSO_4$	169.7	171.0 (11)

NITROGEN

Sample	BE (eV; ± 0.1 eV; level $1s_{1/2}$)
NH_3	399.4

MERCURY

Sample	BE (eV; ± 0.1 eV; level $4f_{5/2,7/2}$)
Hg**	104.4 (5/2) 100.5 (7/2)

* SO_2 aged on uncoated Nuclepore filter

** Calibrant Si $2s_{1/2}$; 152.5 eV

S_8, SO_2, and SO_3^{2-}. In addition, it was noted that the photopeaks for SO_2 collected on the filter papers changed with time, that is, on aging. The measured values are in general agreement with values published by other workers as noted in Table VII. However, where our values differ from those reported by others, this probably results from the use of different calibration standards.

Typical photoelectron spectra (20 eV scans) for sulfur in SO_4^{2-}, SO_3^{2-}, SO_2, and S dusted or adsorbed on uncoated filters are shown in Figures 11-16. In all of these spectra the unresolved $2p_{1/2,3/2}$ doublet of sulfur is evident. The slight shoulder toward high binding energies as noted for sulfur in SO_4^{2-} (Fig. 11) and in other spectra is due to the S $2p_{1/2}$ level while the main peak arises from the $2p_{3/2}$ level. Examination of Figures 12 and 13 clearly illustrates the ease with which sulfur in different oxidation states in mixtures can be detected with the ESCA technique. ESCA is the only analytical technique available today capable of establishing the chemical (bonding) state of elements. In the sulfur spectrum of mixed $FeSO_4$ and ZnS (Fig. 12) and in the mixture of Na_2SO_4 and HgS (Fig. 13), the photopeak at high binding energy is due to sulfate, SO_4^{2-}, while that at lower binding energies is due to sulfide, S^{2-}. The variation in binding energies (see Table VII) for sulfide in ZnS versus CdS or HgS may be due to differences in crystal potential at the sulfide lattice site and/or to the difference in covalent bonding between ZnS versus CdS or HgS.

Examination of Figure 14 reveals that for sulfur in sulfite, SO_3^{2-}, two different photopeaks are observed. One peak has a maximum centered

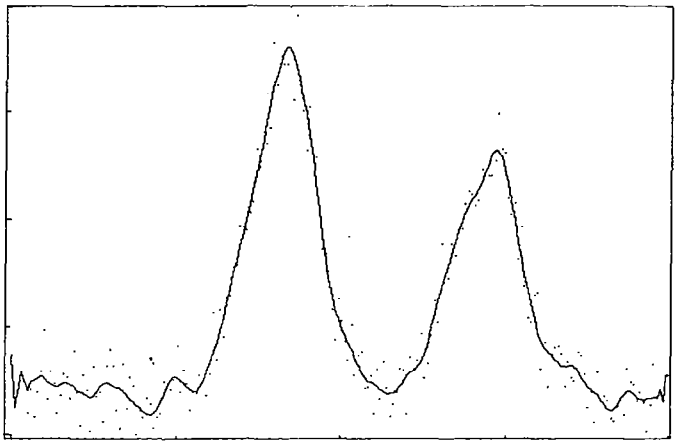

Fig. 12. S 2p Photopeak - $FeSO_4$ + ZnS/74A

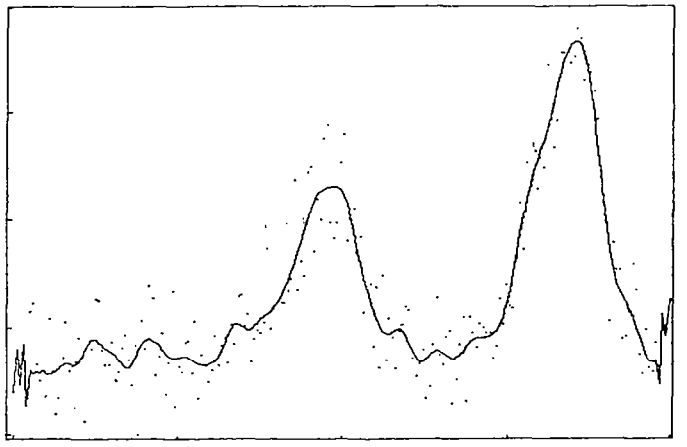

Fig. 13. S 2p Photopeak - Na_2SO_4 + HgS/74A

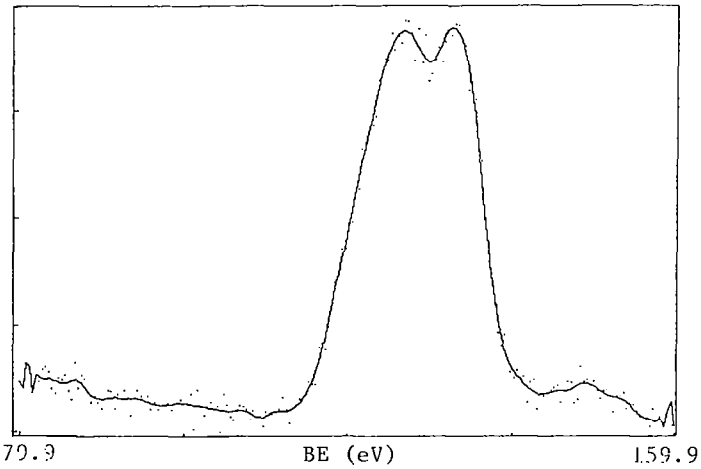

Fig. 14. S 2p Photopeak - Na_2SO_3/74A

at 168.2 eV while the other is at 166.6 eV. It was noted experimentally that the peak at high binding energy increased with time of exposure in the ESCA instrument. This observation may be indicative of in-situ photoinduced oxidation of SO_3^{2-}. It might be expected that the oxidation would proceed to SO_4^{2-}. However, the binding energy for the second peak is lower than that measured for sulfate. This second photopeak at higher binding energy must, therefore, correspond to some sulfur species with a charge density at sulfur intermediate between that of sulfite and sulfate.

In Figure 15 the sulfur spectrum of SO_2 freshly collected on uncoated Nuclepore filters is presented. In this spectrum one well defined peak is noted at a binding energy of 167.5 eV. This value is somewhat lower than the value reported by Novakov (9). This could be due to the fact that our measurement was made on SO_2 freshly adsorbed (not aged) on Nuclepore filters (see discussion below). It is noted that the binding energy for sulfur in SO_2 is higher than that for sulfur in SO_3^{2-}, although both sulfurs are in the +4 oxidation state. This apparent discrepancy is resolved when it is realized that the binding energy is affected by the lattice potential and the net charge on the species in which the sulfur is found. The binding of sulfur in SO_3^{2-} is lowered relative to that in SO_2 because the lattice potential for ionic Na_2SO_3 is greater than that for SO_2 adsorbed on the Nuclepore filter and because the net charge on the SO_3^{2-} ion is negative which would tend to lower the binding energy of sulfur in SO_3^{2-} compared to SO_2 . It is also noteworthy that the binding energy for sulfur in SO_3^{2-} is lower than that measured in SO_3^{2-}

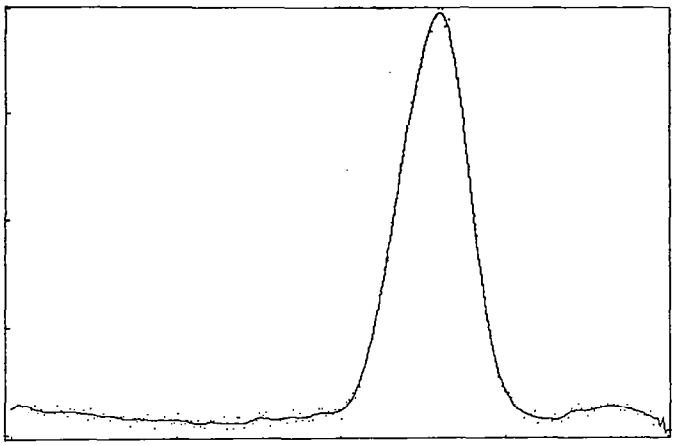

Fig. 15. S 2p Photopeak - SO_2/74A

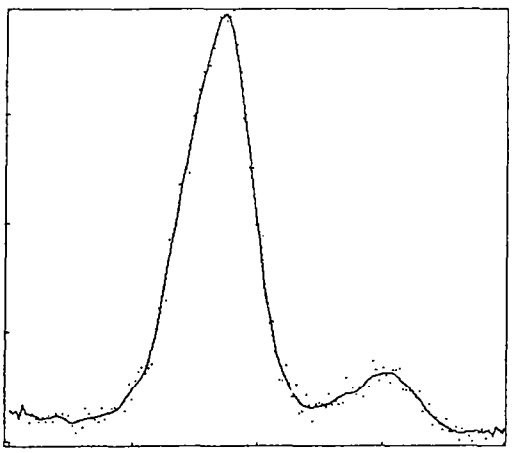

Fig. 16. S 2p Photopeak - SO_2/74A (Aged)

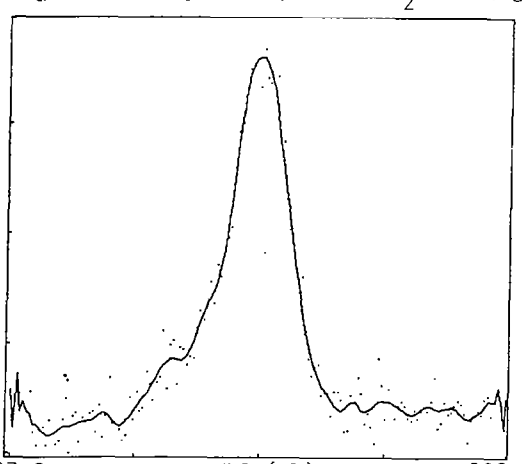

Fig. 17. N 1s Photopeak - NH_3/74A

by Novakov (9). The lattice potential and species charge factors also are responsible for this difference in binding energy for SO_3 and SO_3^{2-}.

In Figure 16 the sulfur spectrum of the SO_2-Nuclepore filter sample after aging is shown. The aging process consists of allowing the sample to sit in the air for about three weeks. From the data in Table VII and Figure 16 it is evident that SO_2 is apparently reacting with the paper or species in the laboratory air. The higher binding energy peak has shifted from 167.5 eV to 168.3 eV and a new peak characteristic of sulfide has "grown in" at 163.4 eV. It is interesting to note that the sulfur at 168.3 eV in aged SO_2 has the same binding energy as the unidentified high binding species noted in sulfite, SO_3^{2-} (cf Fig. 14).

These results suggest that SO_2 may be undergoing several reactions while adsorbed or trapped on the paper. One reaction would be some oxidation of SO_2 by air or reaction of SO_2 with the paper itself. The formation of a lower binding energy species indicates that SO_2 may also act as an agent to oxidize elements in the paper, perhaps $Fe^{2+} \rightarrow Fe^{3+}$. It is also possible that SO_2 on the paper may react with sulfides in the laboratory air and potentially form thiosulfate, $S_2O_3^{2-}$. The binding energies of sulfur in thiosulfate have been measured to be 168.5 and 162.5 eV corresponding to S^{6+} and S^{2-}, respectively. The measured higher binding energy value for $S_2O_3^{2-}$ is close to that measured for the unknown sulfur in the sulfite and in aged SO_2 spectra. This result may be interpreted to suggest that the new sulfur species is $S_2O_3^{2-}$. It should be recognized that this is only one possibility and that various other sulfur species including hydrated and dehydrated SO_2 could be responsible for this unknown sulfur photopeak.

b. Nitrogen

The binding energy for only a single nitrogen-containing species, NH_3, was measured in this work. THe binding energy is given in Table VII and the spectrum is shown in Figure 17. The measured binding energy for NH_3 is somewhat higher than that measured by Jolly and co-workers (12) for solid NH_3. This difference is not unexpected when it is realized that in the NH_3 experiments for this study ammonia was passed over water. It does not correspond to anhydrous NH_3 as does the value reported earlier (12). The binding energy value for NH_3 on the filters is lower than that reported (12) for the ammonium nitrogen in NH_4NO_3 at 402.3 eV. It may be suggested that the value measured on the filter paper corresponds to that for hydrated NH_3 or perhaps for NH_4OH. No alteration in the nitrogen photopeak was observed during the measurements or upon aging. It is evident, therefore, that the ammonia does not react with the paper under the conditions of the experiments.

c. Mercury

In preliminary studies of NASA gold coated filters, evidence was obtained which suggested that mercury was present on the papers. In an effort to determine the binding energy for mercury, elemental mercury was collected on an uncoated Nuclepore filter. Careful examination of the experimental photoelectron spectrum, calibrated using Si $2s_{1/2}$ indicated that (i) the major photopeak at about 101 eV is wider than that previously measured (25) for elemental mercury and mercury in simple compounds, and (ii) the intensity ratio for the two peaks is not characteristic of mercury. The reason for these apparent anomalies is that

the spectrum is a composite spectrum containing photopeaks due to Hg $4f_{5/2}$, $4f_{7/2}$, and Si $2p_{1/2,3/2}$. The silicon peaks arise from the Nuclepore filter paper. In order to establish the absolute binding energy of mercury and silicon the spectrum was deconvoluted using the GASCAP IV routine (26). A fit of the experimental spectrum is shown in Figure 18 while the individual components making up the multiplet are shown in Figure 19. In Figure 19 the peaks at lower and higher binding energies are the Hg $4f_{7/2}$, Hg $4f_{5/2}$ levels, respectively, while the center peak is that due to the Si $2p_{1/2,3/2}$ level. The binding energy 101.5 eV for Si in the deconvoluted spectrum is in excellent agreement with that measured in the blank paper, BE = 101.7 eV. The binding energy values for the mercury levels collected in Table VII are somewhat higher than that determined (25) for mercury amalgamated in gold. This is as expected since it is likely that binding energy of mercury amalgamated with gold possibly would be lower than that for free elemental mercury. In studies (27) of the aluminum binding energies in gold-aluminum alloys, it was observed that the Al binding energy decreased as the % Al in the gold increased. This is consistent with our observation of the lowering of the Hg binding energy upon amalgamation with gold.

4. Elemental analysis and chemical identity of particulates on NASA Samples

The complete summary of the data for NASA samples is given in Table IV. In this section, discussion of each individual sample and the interpretation of the results are presented. ESCA spectra were measured for sulfur and nitrogen in all samples and on elements shown by NAA to be present at levels greater than about 300 ppm. The 300 ppm limit was dictated by

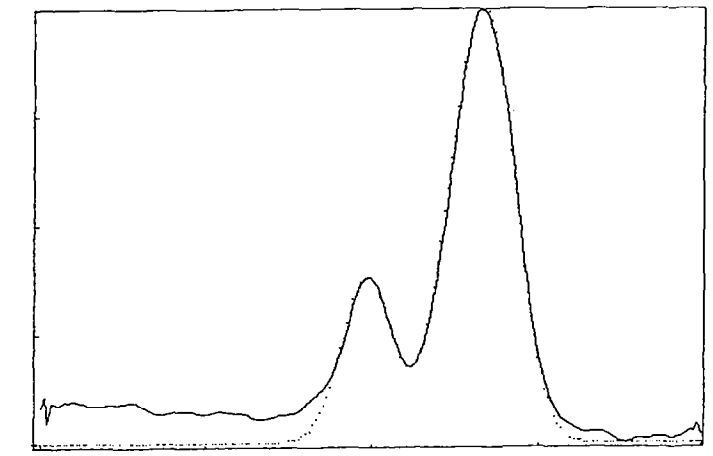

Fig. 18. Hg 4f, Si 2p Photopeak - Hg/74A - Raw Data and Deconvolution Fit

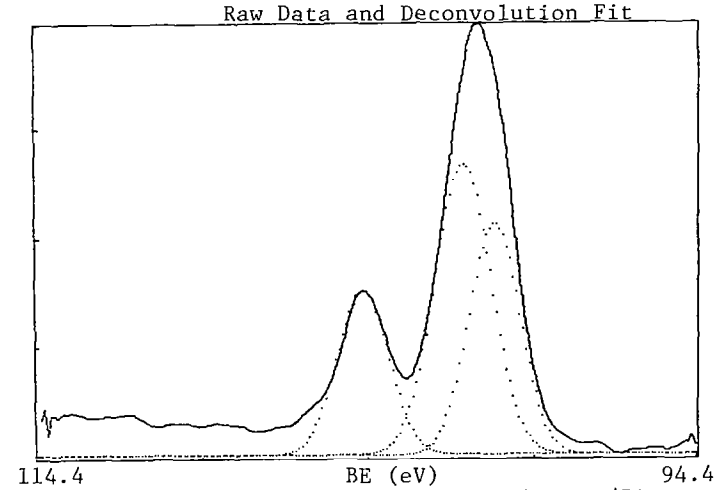

Fig. 19. Hg 4f, Si 2p Photopeak - Hg/74A - Raw Data and Deconvoluted Components

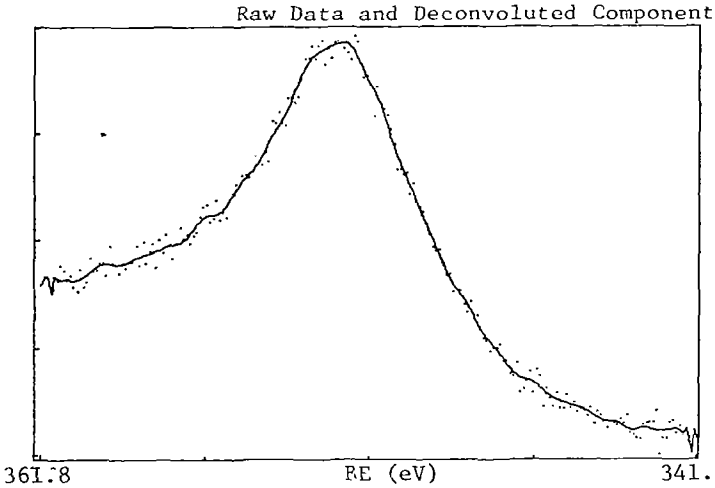

Fig. 20. Ca 2p Photopeak - NASA 1

the fact that concentrations < 300 ppm resulted in excessively long scan times for ESCA analysis. Gold and silicon levels were used in the calibration.

a. NASA 1

The spectrum for calcium obtained for this sample is shown in Figure 20. The binding energy of 352.8 eV is characteristic of Ca^{2+}. Photoelectron spectra also were measured for sulfur, nitrogen, aluminum, chlorine, and cadmium. None of the elements was present in detectable quantities. The Si $2p_{1/2,3/2}$ spectrum is shown in Figure 21. Although the silicon binding energy is slightly less (0.2 eV) than that measured on a blank filter paper, it is probable that the Si peaks are due primarily to the paper. However, the presence of silicate particulate matter cannot be ruled out.

Examination of the binding energy region 110 to 90 eV over a period of time revealed an interesting phenomenon on the gold coated filters. In Figure 22 is shown the Si $2p_{1/2,3/2}$ region for a fresh gold coated NASA Nuclepore filter (NASA 38A). This spectrum is similar to that determined for Si on unocated filters. The binding energy, 101.6 eV, calibrated vs gold is also in excellent agreement with that measured for uncoated filters. This spectrum (Figure 22) provides an indication of the nature of the Si $2p_{1/2,3/2}$ photopeak for fresh, unexposed gold coated paper. In Figure 23 is shown the spectrum of NASA 1 in the Si $2p_{1/2,3/2}$ region measured three months after that measured in Figure 21. The obvious result is that some additional material has been deposited on the paper and that the single Si $2p_{1/2,3/2}$ peak has disappeared. Careful measurement of the binding energies for these two peaks, using the Si

Fig. 21. Si 2p Photopeak - NASA 1

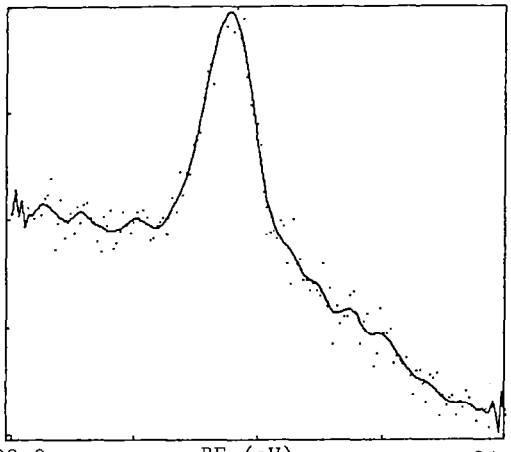

Fig. 22. Si 2p Photopeak - NASA 38A

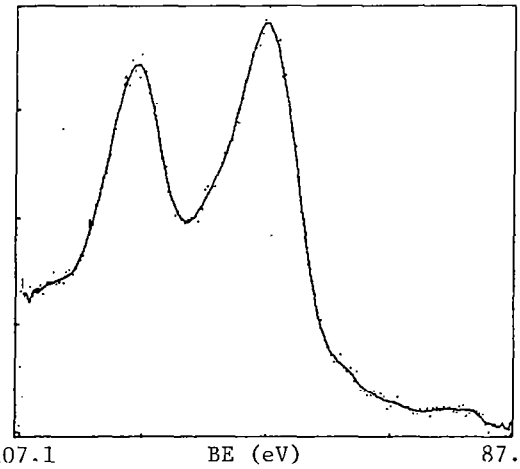

Fig. 23. Hg 4f, Si 2p Photopeak - NASA 1

$2s_{1/2}$ level at 152.5 eV, gave values of 103.5 and 99.7 eV for the least abundant and the most abundant peaks, respectively. Comparison of these values with values measured for elemental mercury amalgamated with gold (25), BE's 103.3 and 99.2 eV strongly suggests that the filter has picked up mercury in the laboratory environment. This NASA 1 sample and all other NASA samples were placed in polyethylene petri dishes and housed in a cardboard box when not under investigation. These unexpected results, while not an objective of this research, suggest the utility of ESCA as a monitoring technique in the quantitative analysis of mercury collected on gold coated Nuclepore filters.

b. NASA F-2

The elements detected in NASA F-2 samples were silicon, sulfur, nitrogen, and calcium. The spectra for sulfur and nitrogen are shown in Figures 24 and 25, respectively. Other elements for which ESCA scans were made, but for which no detectable signal was obtained, are listed in Table IV. The silicon photopeak was characteristic of that for Si in the paper. The sulfur peak, Figure 24, and the measured binding energy, 167.9 eV, is consistent with the identification of sulfur as SO_2. The binding energy for sulfur in SO_2 measured in this study is 167.5 eV while that measured by Novakov (10) is 167.9 eV. Our own measurement for freshly deposited SO_2 is lower than that on the NASA sample, but it was noted (Section 3) that upon aging, the binding energy of SO_2 on uncoated paper increased. It is possible that the difference between NASA F-2 and our own measurement is the result of this aging process. If aging is responsible for the difference, then aging on the gold coated paper

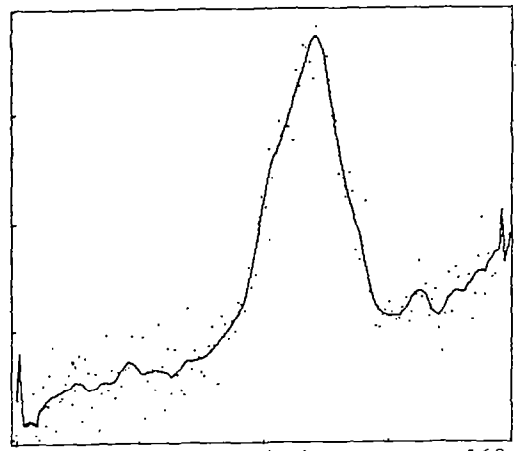

Fig. 24. S 2p Photopeak - NASA F-2

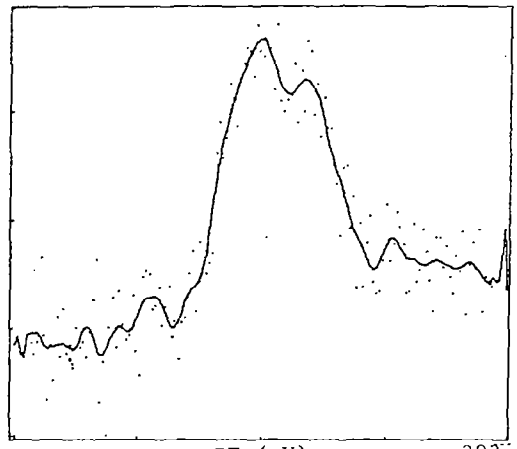

Fig. 25. Ti 1s Photopeak - NASA F-2

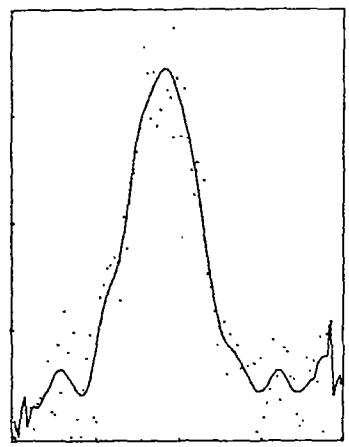

Fig. 26. S 2p Photopeak - NASA 4

must be much slower since the NASA F-2 sample is much older (2 years) than our freshly deposited SO_2 sample.

The spectrum of the N $1s_{1/2}$ level in NASA F-2 (Fig. 25) shows two moderately resolved peaks at 400.8 eV and at 399.4 eV. Upon comparison of the lower binding energy value with that for NH_3 on an uncoated paper, BE = 399.4, it is evident that the lower photopeak is due to either ammonia or to an amine. The higher binding energy peak is indicative of a more positive nitrogen. Since no nitrogen standards, other than ammonia were measured in this study it is only possible to speculate on the nature of this nitrogen. If the structure is organic in nature, it must contain an electron withdrawing group adjacent to nitrogen so as to reduce the electron density on nitrogen. Groups which could affect this would be carbonyl, $>C=O$; nitro, $-NO_2$; or ester groupings $R-O-\underset{|}{C}=O$. The nitro groups can be quickly eliminated since no N $1s_{1/2}$ photopeak was noted at a binding energy of about 402-407 eV (12). Neither the carbon nor the oxygen regions were measured in these studies so the presence of any carbon or oxygen cannot be supported. Additional inorganic nitrogen-containing species, NO, N_2O, N_2H_4, NH_2OH, could be responsible for the nitrogen species at 400.8 eV. However, no definitive assignment can be made unless the measurements for these standard materials are carried out.

In addition to the non-metals, calcium was detected in NASA F-2 and was presumably present as Ca^{2+}. As with NASA 1, prolonged storage of NASA F-2 results in the accumulation of mercury on the gold coated paper. The Si $2p_{1/2,3/2}$ spectrum of NASA F-2 was measured 3 1/3 months after initial analysis and again peaks due to elemental mercury were present on either side of the central Si $2p_{1/2,3/2}$ photopeak.

c. NASA 4

ESCA spectra obtained for significant elements (S, N, Si, and Ca) detected in NASA 4 include Figure 26 for sulfur and Figure 27 for nitrogen. The binding energy of the sulfur peak (Fig. 26) is 168.2 eV. The binding energy for this sulfur is characteristic of the unidentified sulfur in SO_3^{2-} and in aged SO_2 standard samples. It was mentioned (Section 3) that this unknown peak is possibly thiosulfate.

The nitrogen spectrum (Fig. 27) is indicative of an amount of ammonia or amines at BE = 399.7 eV, and a larger amount of the more highly positive nitrogens at BE = 401.1 eV. As noted for NASA F-2, this higher photopeak could be due to amide type nitrogen or the presence of a variety of nitrogen oxides.

The silicon $2s_{1/2}$ spectrum was similar to that obtained for other samples. The Si $2p_{1/3,3/2}$ spectrum had photopeaks again characteristic of both silicon and mercury. Although scans for Pb, Na, Mg, Cd, and Ca were made, only calcium was detected. The measured binding energy was equivalent to that determined on other samples and corresponds to Ca^{2+}.

d. NASA F-12

The elements and the particular species detected on the NASA F-12 sample are virtually identical with those noted in NASA F-2. The one exception is that mercury was also detected in NASA F-12. The sulfur species shown in Figure 28 with a binding energy of 167.8 eV is characteristic of SO_2. The nitrogen spectrum, shown in Figure 29 shows two peaks characteristic of ammonia and/or amines and oxidized more positive nitrogen, N_2O, NO, amides, etc. The silicon $2p_{1/2,3/2}$ spectrum showed

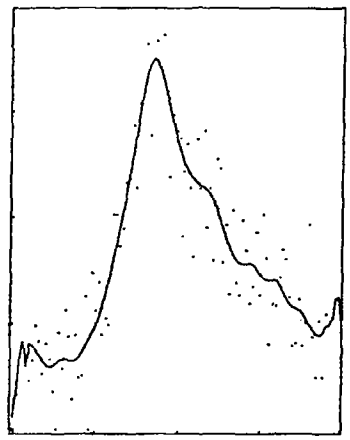

405.3 BE (eV) 395.3

Fig. 27. N 1s Photopeak - NASA 4

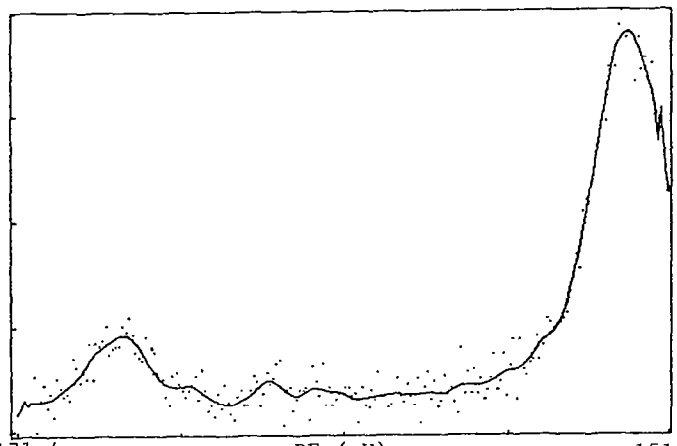

171.4 BE (eV) 151.4

Fig. 28. S 2p, Si 2s Photopeak - NASA F-12

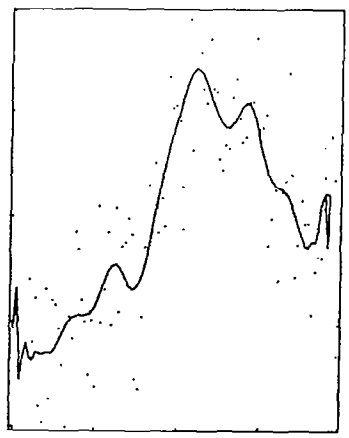

406.4 BE (eV) 396.4

Fig. 29. N 1s Photopeak - NASA F-12

the presence of silicon from the paper, and mercury. Aluminum was not detected. Calcium was detected and presumably is present as Ca^{2+}. Other elements for which spectra were measured but showed no detectable signal are noted in Table IV.

e. NASA 13

In the NASA 13 sample the elements, sulfur, nitrogen, chlorine and sodium were noted. Neither calcium nor mercury was noted in this sample. It is significant that NASA 13 was an uncoated filter and therefore not susceptible to contamination by mercury. The spectrum for sulfur in Figure 30 is characteristic of sulfate and has a binding energy of 169.3 eV. This value is in fair agreement with that measured for sulfate in $FeSO_4$ and Na_2SO_4 (see Table VII).

The nitrogen spectrum in Figure 31 shows two unresolved peaks with binding energies of 399.7 eV and a shoulder at 398.4 eV. The higher binding energy value is characteristic of ammonia or amines, while the lower value is consistent with the presence of a cyano group, i.e., HCN or CH_3CN, etc. The measured binding energy is similar to those noted by Jolly (12) for simple -CN containing compounds: i.e., C_6H_5CN, 398.4; KSCN, 398.5; KOCN, 398.3; and KCN, 399.0 eV. To confirm this suggestion additional measurements of the appropriate standards should be carried out.

The Si $2p_{1/2,3/2}$ spectrum showed a clear single photopeak characteristic of an uncontaminated sample. It is evident from this data that no mercury is present in this sample and thus interference from mercury is not expected on uncoated filters.

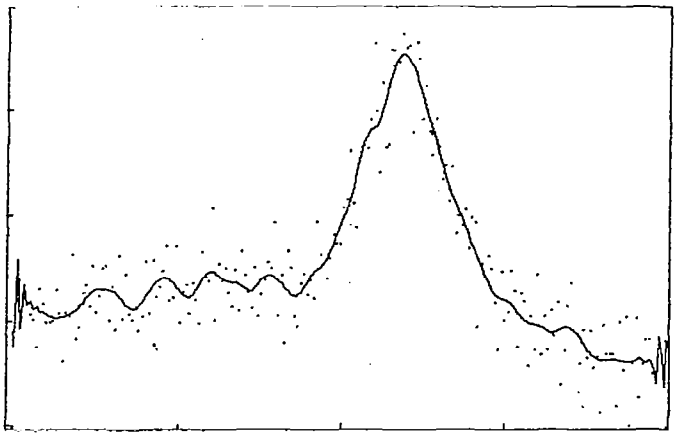

Fig. 30. S 2p Photopeak - NASA 13

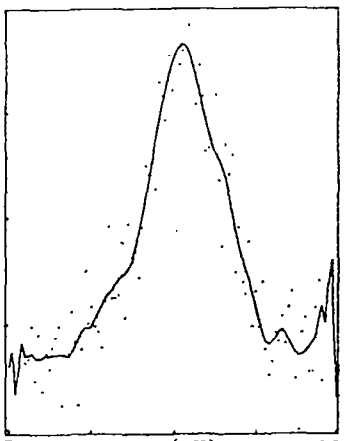

Fig. 31. N 1s Photopeak - NASA 13

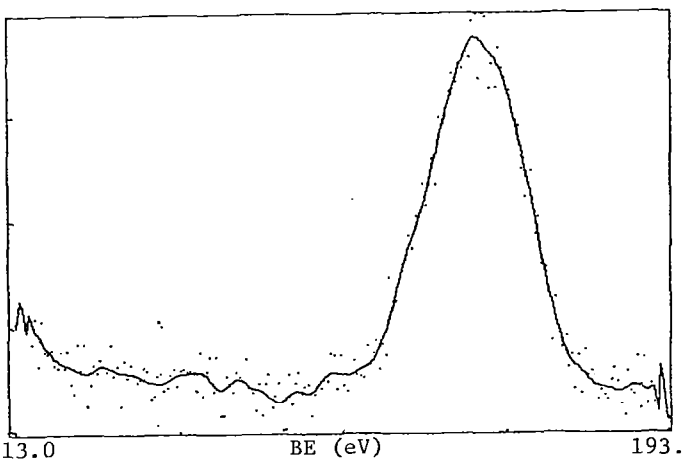

Fig. 32. Cl 2p Photopeak - NASA 13

A survey of spectra for Ca, Cl, and Na indicate that calcium is absent while chlorine and sodium were present as seen in Figures 32 and 33. The chlorine present as Cl^- in the sample is identified by comparison of binding energies (25) for chloride in simple metal halides. Sodium is present as Na^+.

PART 2. NASA-KENNEDY SPACE CENTER SAMPLES

A. Neutron Activation Analysis (NAA)

The NAA results for the test samples are summarized in Table VIII. Although complete NAA analysis were carried out, only the elements found in the largest quantity are presented in Table VIII. The data for aluminum, which is of particular interest for this work, has (according to K. H. Crumbly) been corrected for interference from silicon. This silicon-containing material is apparently incorporated into the fibers in the manufacturing procedure.

The NAA results indicate that aluminum is present, but less than 20 µgms of aluminum was detected in any one filter sample. The values for Al in Table VIII are expressed as µgm of Al on the filter and the values in brackets are expressed as ppm Al (Al wt./total post launch filter wt.). The results further indicate that the amount of aluminum collected during launch was not greater than 20 µgm while the amount of aluminum was about 3 µgm when collected during 24 hours of launch inactivity. The aluminum content for both background samples, 75-A-179 and 75-A-181 is approximately the same for collection over a 24 hour period. The level of aluminum found in the two ocean vessel collected samples, 75-A-20 and 75-A-21, is also about the same but less than that for aluminum collected

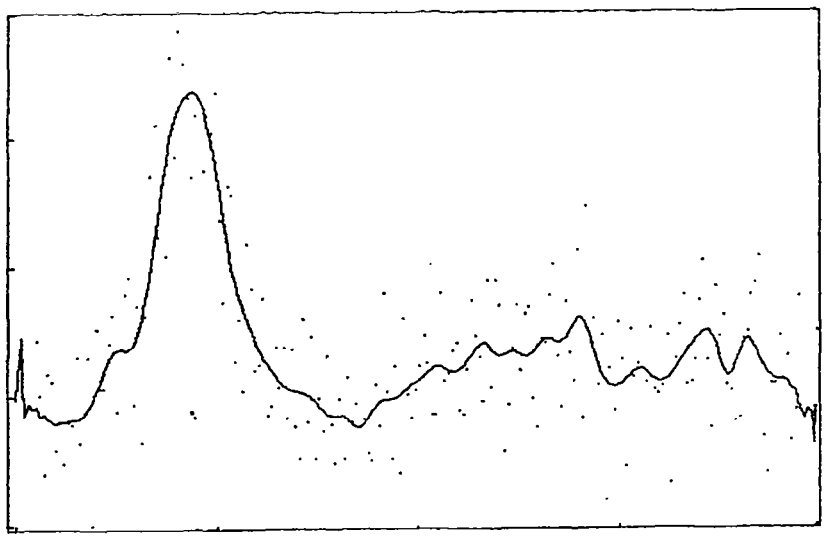

Fig. 33. Na 2s Photopeak - NASA 13

TABLE VIII

SUMMARY OF NAA RESULTS FOR NASA-KSC SAMPLES

(Launch and Background Sampling)

Sample	Al	Br	Ca	Cl	Cr	Cu	Fe	K	Mg	Na	S	Sn
75-A-20(P-4)	1.84* [185]**	0.15	2.1	1.19	5.9	0.14	37	1.0	0.8	2.6	23	1.1
75-A-21(P-2)	1.34 [134]	0.73	1.2	1.24	4.5	0.25	32	0.77	0.91	2.55	--	1.3
75-A-41(A-1)	16. [1600]	0.11	3.0	1.74	5.1	0.04	27	1.68	4.1	2.43	27	1.1
75-A-47(A-7)	4.7 [490]	--	0.7	0.64	4.9	0.06	22	--	--	1.1	--	0.8
75-A-161(S204)	2.03	0.005	--	0.61	0.015	0.026	8.5	0.15	0.53	0.45	--	--
75-A-174(P-4)	7.68 [1023]	0.009	1.0	3.33	0.036	0.032	3.3	0.24	0.98	0.92	--	0.06
75-A-179	2.47 [328]	0.22	2.2	1.22	0.16	0.47	11	2.61	2.0	8.9	--	0.12
75-A-181	2.74 [370]	0.22	5.0	5.04	0.16	0.21	7	1.81	2.98	15.0	--	0.10

* Concentrations expressed in μg

** Bracketed concentrations expressed in ppm Al (wt. Al/wt. post launch filter)

on any of the other filters. The highest aluminum level was found in filters 75-A-41 and 75-A-47. These samples were the aircraft-collected filters and would be expected to contain high levels of aluminum. The aluminum content for the remaining filters, 75-A-161 and 75-A-174, is less than that for the aircraft filters but greater than that for the ocean vessel samples. The 75-A-161 and 75-A-174 samples were obtained during collection for approximately three hours at ground stations in the launch area before an aborted launch. The aluminum content from these ground samples does however appear questionable, since aluminum was not detected using ESCA. SEM photomicrographs indicated that there were no detectable particles on the filters. The NAA results show that aluminum is present in the aircraft-, ocean vessel-, and background-collected sample filters. The levels of Al in these samples are significantly below those levels that were first considered as being detectable using ESCA. As will be pointed out later in this report, aluminum at these levels could be detected and chemical-identity information could be obtained by ESCA for these aluminum-containing filters.

B. Scanning Electron Microscopy (SEM)

The SEM photomicrographs were used to determine on which side of the filter atmospheric sample particles had been collected. The results of this study are presented in Table I and the SEM photomicrographs are presented in Figures 34-41.

Examination of filters 75-A-20, 21 shown in Figures 34 and 35 respectively, reveal that the filters are covered to an extent of about 10-15% (area) by small spherical-looking particles. These 2000X portions are representative of the whole filter. Additional SEM Photomicrographs

Fig. 34. SEM Photomicrograph (2000X) - NASA 75-A-20

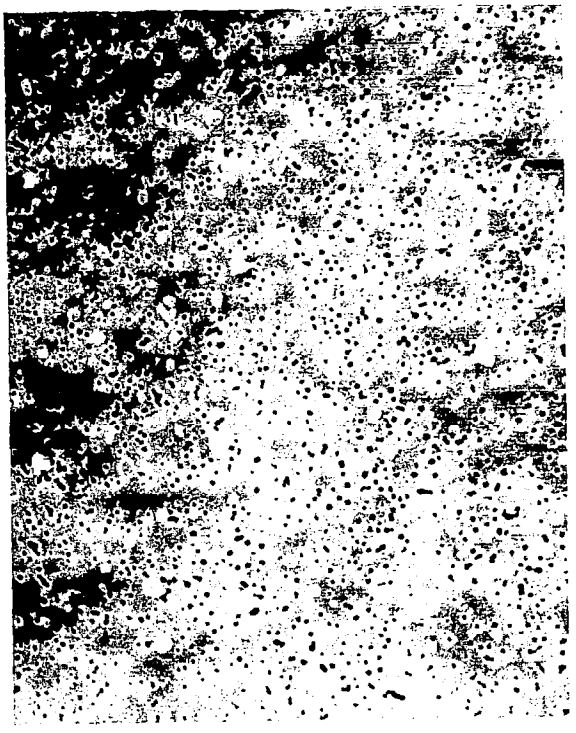

Fig. 35. SEM Photomicrograph (2000X) - NASA 75-A-21

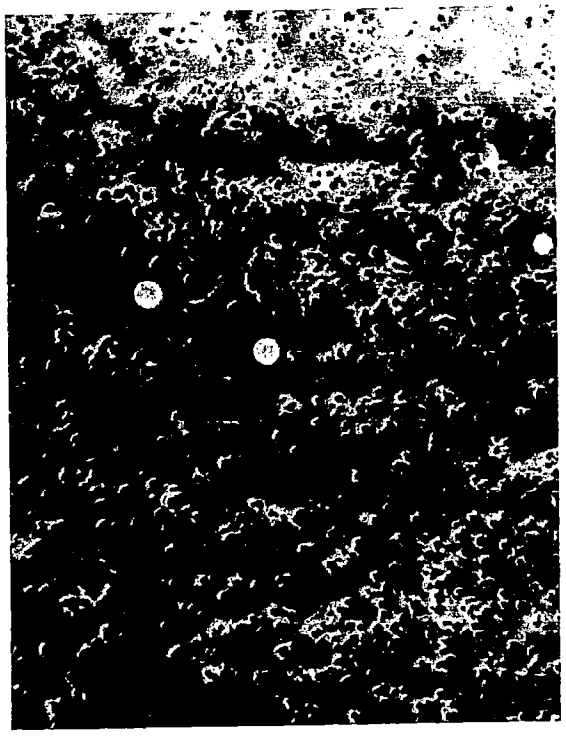

Fig. 36. SEM Photomicrograph (2000X) - NASA 75-A-41

Fig. 37. SEM Photomicrograph (2000X) - NASA 75-A-47

at lower magnification and in other areas of the filter show similar features and approximately the same number of particles as shown in Figures 34 and 35. On filters 75-A-20 and 75-A-21 the particle size ranges from 2.5 to about 0.25 μm. However, the number of particles in 75-A-21 is greater than that for 75-A-20. The particles that are unique in these figures and which appear to be characteristic of the rocket exhaust particulates are the larger (2.5×10^{-3} μm) spherical particles. It should be noted that no particles appear in Figures 34 and 35 with characteristics similar to those of pollen, dirt, or other "background" materials observed in the Norfolk samples (cf Figure 2) or in the background samples (cf Figures 40 and 41) collected for this study. Thus, it can be suggested that the particles collected on filters 75-A-20 and 75-A-21 are characteristic of launch activities. In rocket exhausts, the aluminum particulate matter is reportedly (28) identified as Al_2O_3. The Al_2O_3 particulate matter appears as irregular spheres that are approximately 5 μm in diameter.

The SEM pictures of filter samples 75-A-41 and 75-A-47 (Figures 36 and 37), collected via air craft flights through the rocket exhaust cloud, reveal only a scant number of small ($\tilde{\sim}$ 2μm) spherical particles. The size and shape of the particles are the same in both photographs. From the SEM photographs, it appears that a greater number of particles was collected on filter 75-A-47 than on filter 75-A-41. Study of these filters at lower magnifications confirms this suggestion. This conclusion is in direct contrast to the NAA results.

The SEM results for filters 75-A-161 (S204) and 75-A-174 (P4) are presented in Figures 38 and 39. From these photos it is apparent that no

Fig. 38. SEM Photomicrograph (2000X) - NASA 75-A-161

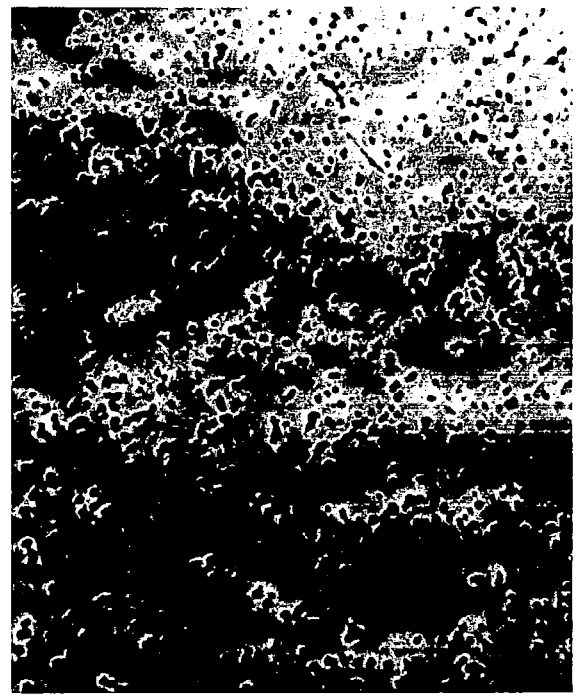

Fig. 39. SEM Photomicrograph (2000X) - NASA 75-A-174

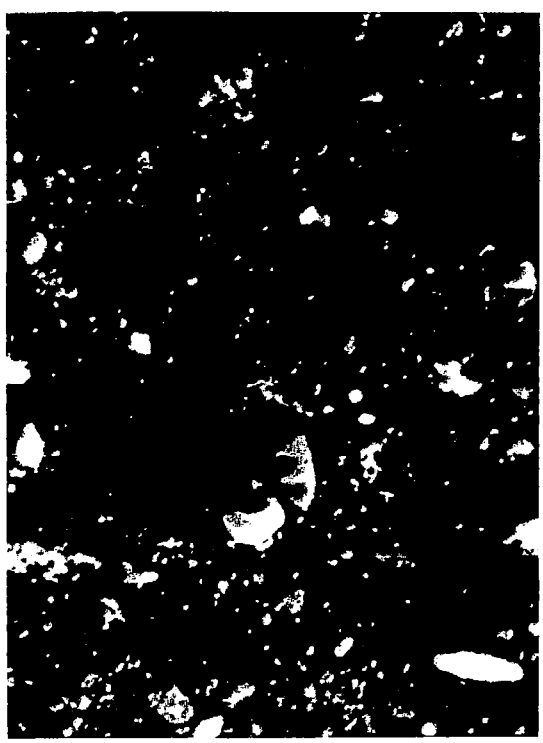

Fig. 40. SEM Photomicrograph (2000X) - NASA 75-A-179

Fig. 41. SEM Photomicrograph (2000X) - NASA 75-A-181

particles are detected with a nature or characteristic similar to those noted in Figures 34-37, or 40 and 41. This result is somewhat surprising since the NAA data (see Table VIII) would suggest that these filters should have a quantity of particles significantly greater than that noted in Figures 34 and 35. The ESCA data also supports the conclusion based on the SEM in that no significant Al photopeak was observed for either of these samples.

The background samples collected for 24 hours during launch inactivity are shown in Figures 40 and 41. These SEM photomicrographs reveal particulate matter similar to that found for the Norfolk samples. Also noted are some particles (although few in number) that are spherical and of approximately the same dimensions as those noted in Figures 34-37. These particles could have originated from rocket exhausts or from other high temperature processes that yield small spherical particles. From this study the source of these background particles cannot be determined.

C. ESCA Analysis

ESCA data were obtained on six uncoated Nuclepore filters used by NASA to collect particles and on uncoated Nuclepore filters upon which standard compounds had been deposited at the VPI&SU laboratory. Determination of the binding energies for standard samples was necessary to aid in the chemical identification of the aluminum species detected on NASA test samples.

The ESCA results are presented in the following sequence:

1. Binding energy results for standard aluminum-containing compounds.
2. Binding energy results for NASA samples.

3. Quantitative aspects of aluminum ESCA data: comparison with SEM and NAA.

1. Binding energy results for standard aluminum-containing compounds.

The binding energies for aluminum $2p_{1/2,3/2}$ (2p) core levels were measured for a number of samples collected on Nuclepore filters. Binding energy data taken from the literature were also collected and, in some cases, remeasured to check for accuracy. The results of this effort are summarized in Table IX. The results fall into approximately three binding energy regions for all samples. These data are presented in the three groups, A, B, and C, to facilitate comparisons between the standard compounds and the NASA filter samples.

Typical aluminum 2p photopeaks are shown in Figures 42-51 for $AlCl_3.\eta H_2O$, α-Al_2O_3, γ-Al_2O_3, α-$Al_2O_3.3H_2O$, α-$Al_2O_3.xHCl$, $\gamma Al_2O_3.xHCl$, Na_3AlF_6, and $Al_2Si_2O_7.2H_2O$. The peaks have a peak width at half maximum (PWHM) of about 1.8-2.0 eV. The peaks are symmetrical and as noted from Table IX, the binding energies vary from values of 76.7 eV to 74.0 eV for this work. Upon comparison of the binding energies measured in this work with those reported by others (18-20) the values for the binding energies are not always in agreement. However, it is noteworthy that the differences in measured binding energies for pairs of compounds are in reasonably good agreement. This comparison of differences indicates that the methods of calibration are internally consistent. However, the lack of agreement between investigators suggests that elimination of charging effects, and other uncertainties in sample handling, influence absolute binding energy measurements. It appears, therefore, that the comparison of absolute binding energies for standard samples and unknown

TABLE IX

ALUMINUM 2p CORE BINDING ENERGIES FOR STANDARD ALUMINUM-CONTAINING COMPOUNDS

Sample	Al,2p BE(eV)*			Reference
	A	B	C	
$AlCl_3$	76.8	75.6	73.4	a**
Al_2O_3	76.7	75.4	73.2	a 20
α-Al_2O_3.HCl		75.5		a
α-Al_2O_3.CO		75.3		a
α-Al_2O_3.$3H_2O$		75.3	74.2	20 a
α-Al_2O_3.H_2O		75.2		20
β-Al_2O_3.$3H_2O$		75.1		20
β-Al_2O_3.H_2O	76.1			20
γ-Al_2O_3		75.7		a
γ-Al_2O_3.HCl		75.5		a
Na_3AlF_6		75.0		a
Al_2SiO_5 (Kyanite)			74.4	18
(Kyanite)			74.3	19
(Sillimanite)			73.0	18
(Sillimanite)			74.3	19
$Al_2Si_2O_7$			74.0	20
$MgAl_2O_4$		75.7		20
$Na_3AlSi_3O_8$ (albite)			73.8	21
$(MgFe)_3Al_2(SiO_4)_3$ (garnet)			74.5	21

* Binding energy values have been corrected for differences in binding energies used for calibration standards.

** This work

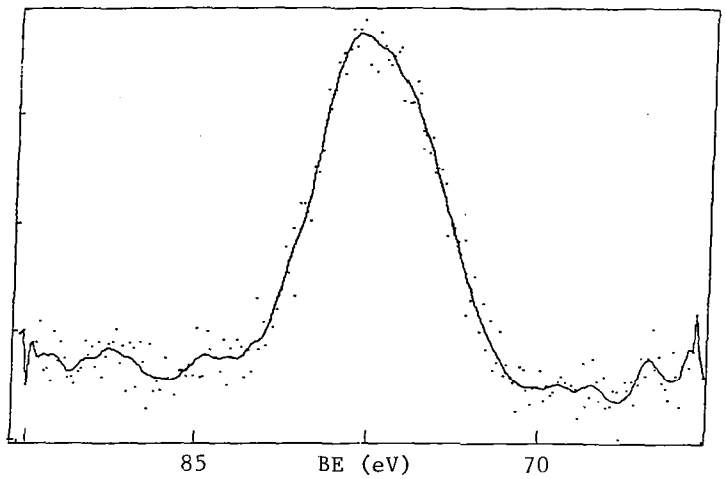

Fig. 42. Al 2p Photopeak - $AlCl_3 \cdot nH_2O$ - Raw Data

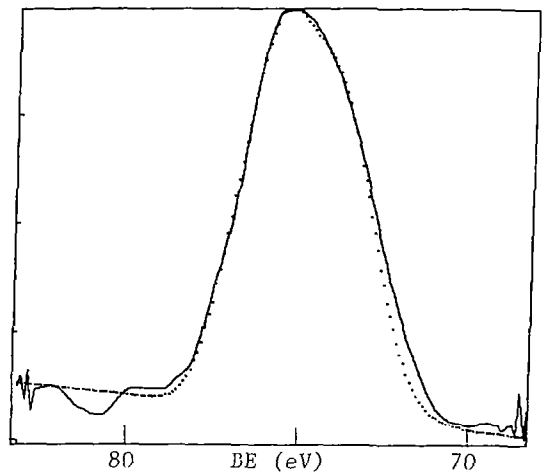

Fig. 43. Al 2p Photopeak - $AlCl_3 \cdot nH_2O$ - Raw Data and Deconvolution Fit

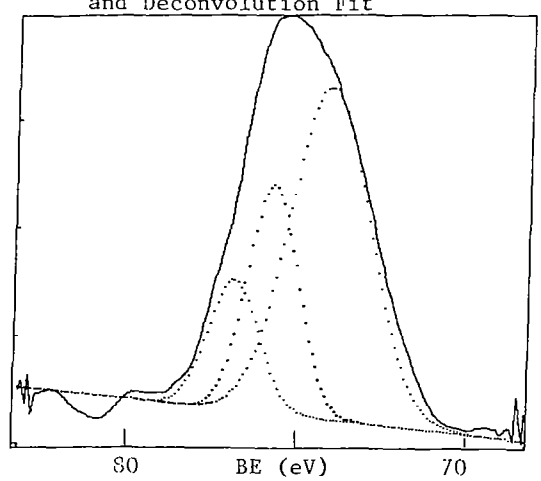

Fig. 44. Al 2p Photopeak - $AlCl_3 \cdot nH_2O$ - Raw Data and Deconvoluted Components

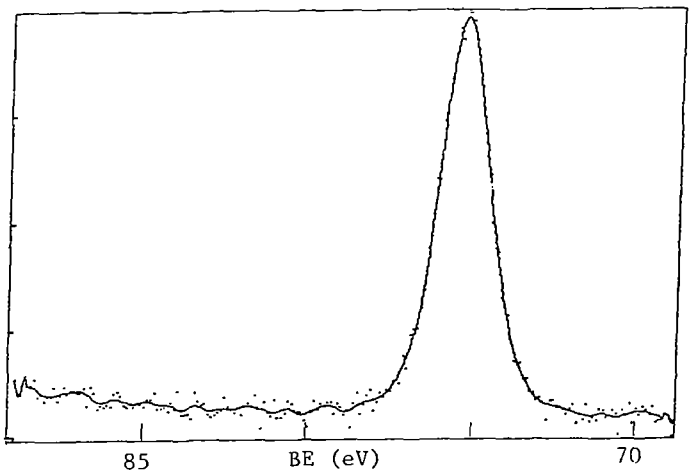

Fig. 45. Al 2p Photopeak - α-Al_2O_3

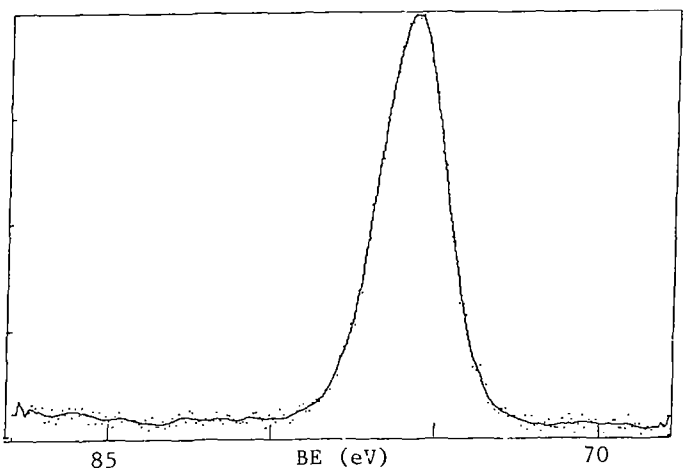

Fig. 46. Al 2p Photopeak - γ-Al_2O_3

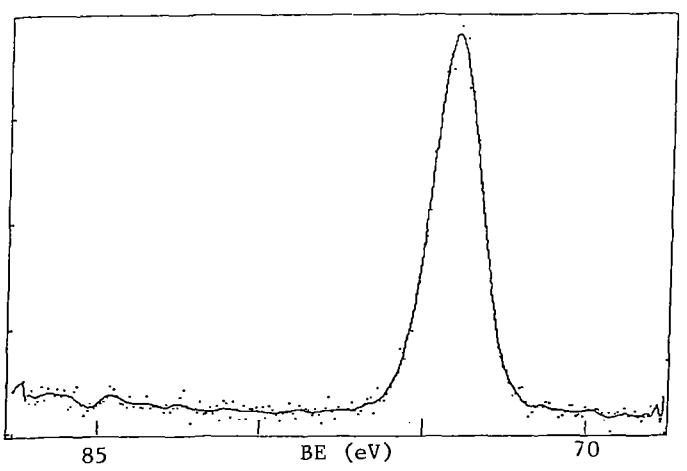

Fig. 47. Al 2p Photopeak - α-$Al_2O_3.3H_2O$

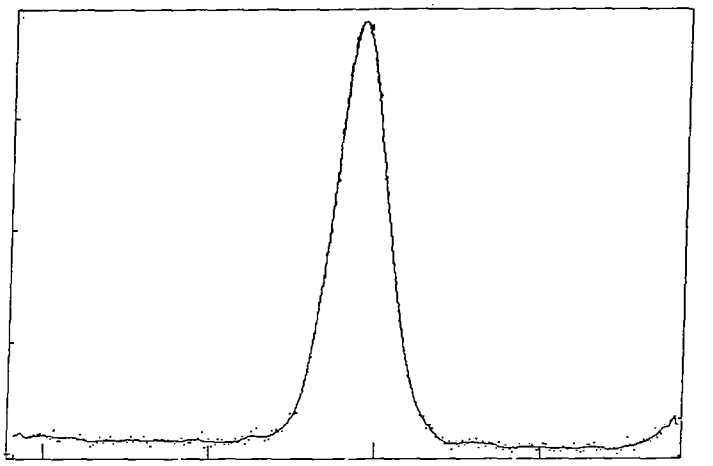

Fig. 48. Al 2p Photopeak - α-Al_2O_3.xHCl

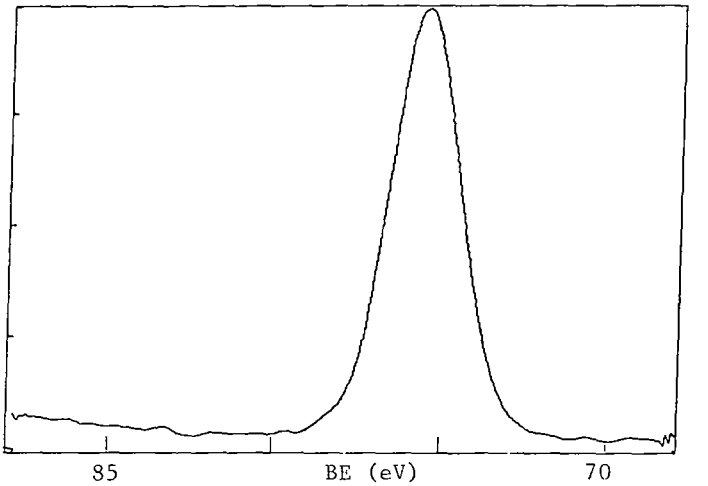

Fig. 49. Al 2p Photopeak - γ-Al_2O_3.xHCl

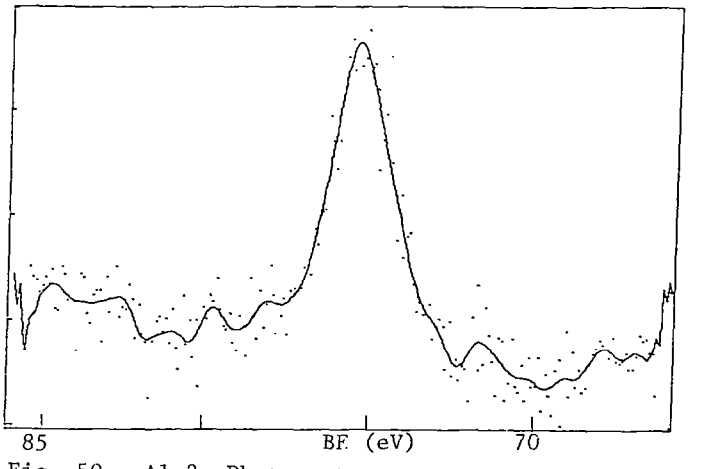

Fig. 50. Al 2p Photopeak - Na_3AlF_6

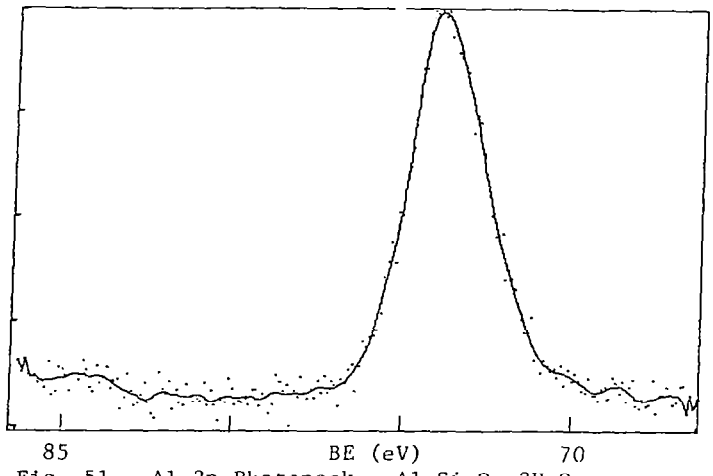

Fig. 51. Al 2p Photopeak - $Al_2Si_2O_7.2H_2O$

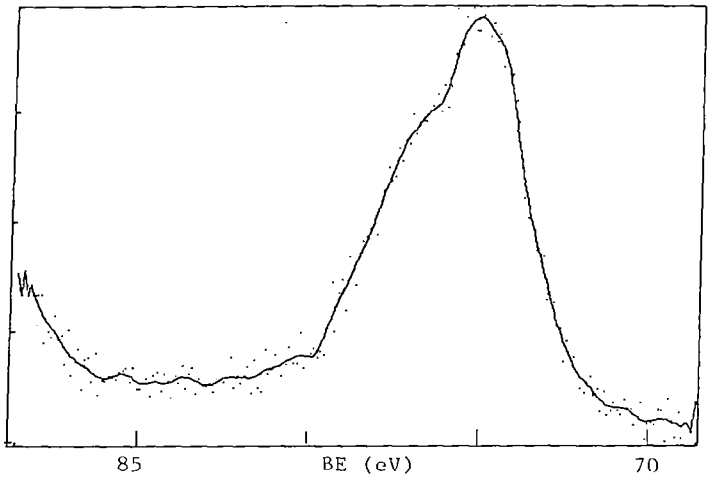

Fig. 52. Al 2p Photopeak - NASA 75-A-20 - Raw Data

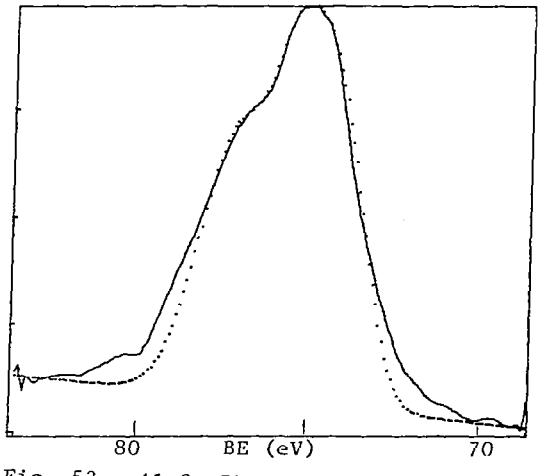

Fig. 53. Al 2p Photopeak - NASA 75-A-20 - Raw Data and Deconvolution Fit

samples should only be made within a given laboratory where calibration procedures are uniform. Nevertheless, comparison of binding energies measured in this study can aid in identifying the aluminum-containing material on the NASA filters. Further comment on the measured binding energies for some of the standard samples is appropriate.

The measured binding energy (BE) for α-Al_2O_3 falls between the values reported earlier (18,20). The BE value for $AlCl_3$ is indicative of $AlCl_3$ which appears to be contaminated with water in the preparation of the sample. The Al 2p peak for $AlCl_3$ shown in Figure 42 is much wider than that for other samples which are known to be "clean" samples. From the $AlCl_3$ photopeak, at least three peaks can be found by deconvolution as seen in Figure 44. In all likelihood these peaks correspond to some pure uncontaminated $AlCl_3$ (high BE), Al_2O_3, and hydrated Al_2O_3. These latter two species would arise from the different hydrolysis products of $AlCl_3$ according to the reactions below.

$$2AlCl_3 + 3H_2O \rightarrow Al_2O_3 + 6HCl$$

$$Al_2O_3 + nH_2O \rightarrow Al_2O_3.nH_2O$$

Comparison of the BE value for α-$Al_2O_3.3H_2O$ with that published earlier (20) reveals that the previous value is higher than that measured here. This discrepancy could be accounted for by incomplete correction for charging in the previous study (20).

In an attempt to determine whether the binding energy for aluminum would be altered by the presence of adsorbed species, e.g., HCl and CO, samples were prepared and the ESCA spectra measured. The Al 2p binding energies for α and γ alumina were equivalent, within experimental error,

with the values for α-Al_2O_3.HCl, α-Al_2O_3.CO and γ-Al_2O_3.HCl. In addition, it was discovered that upon measurement of the ESCA spectra for 2p Cl levels, no increase in the Cl signal was observed. Since it is known that HCl is adsorbed onto Al_2O_3 (29) a likely explanation for detecting no change in the Cl 2p signal level could be that HCl was photodesorbed during measurements of ESCA spectra. It is of interest to note that the binding energy for the Al 2p level measured in this study is lower for α-Al_2O_3.$3H_2O$ than for α-Al_2O_3. This result would be consistent with the notion that water in the Al_2O_3 lattice is effective in increasing the electron density on Al.

The remaining Al 2p binding energies presented in Table IX are representative of aluminum in various minerals. A particularly significant result is that (19) which indicates that the binding energy of aluminum is the same for aluminum in octahedral or tetrahedral coordination.

2. Binding energy results for NASA samples

A summary of the measured (deconvoluted) binding energies for the NASA filter samples is presented in Table X. Representative Al 2p spectra are shown in Figures 52-59. The most striking results from the ESCA data is that filters NASA 75-A-20 and NASA 75-A-47 have Al 2p peak shapes that are approximately the same as shown in Figures 52 and 55. The figures reveal that the PWHM for these Al 2p levels are of the order of 5-6 eV. This is in sharp contrast to the narrow (1.6-2.0 eV) PWHM noted for the clean authentic aluminum-containing standard samples. The interpretation of this result is that several different types of aluminum species are present on the filters. To determine the nature of these species the composite peaks for the NASA samples were deconvoluted into three

TABLE X

ALUMINUM 2p CORE BINDING ENERGIES

FOR NASA-KSC SAMPLES

Type	Sample	Al, 2p BE (eV).		
		A	B	C
Ocean	75-A-20 (P-4)	77.2	75.3	74.1
Ocean	75-A-21 (P-2)	77.4	75.5	73.7
Aircraft	75-A-41 (A-1)	77.0	75.2	73.8
Aircraft	75-A-47 (A-7)	77.0	75.0	73.3
Ground	75-A-161 (S204)	-	-	-
Ground	75-A-174 (P4)	-	-	-
Background	75-A-179	77.1	75.4	73.8
Background	75-A-181	77.0	75.2	73.7

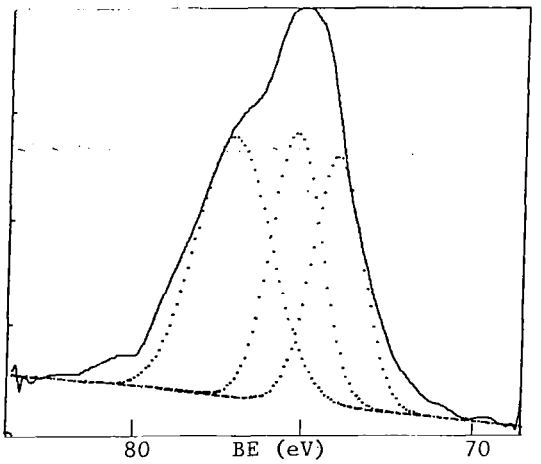

Fig. 54. Al 2p Photopeak - NASA 75-A-20 - Raw Data and Deconvoluted Components

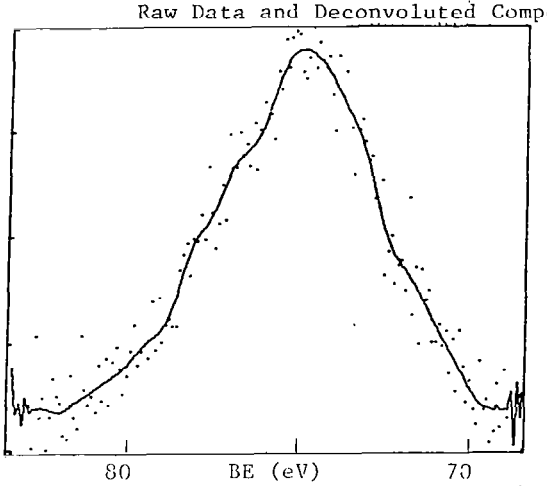

Fig. 55. Al 2p Photopeak - NASA 75-A-47 - Raw Data

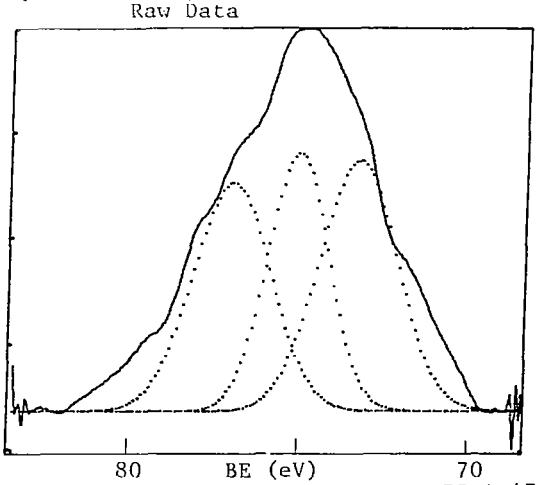

Fig. 56. Al 2p Photopeak - NASA 75-A-47 - Raw Data and Deconvoluted Components

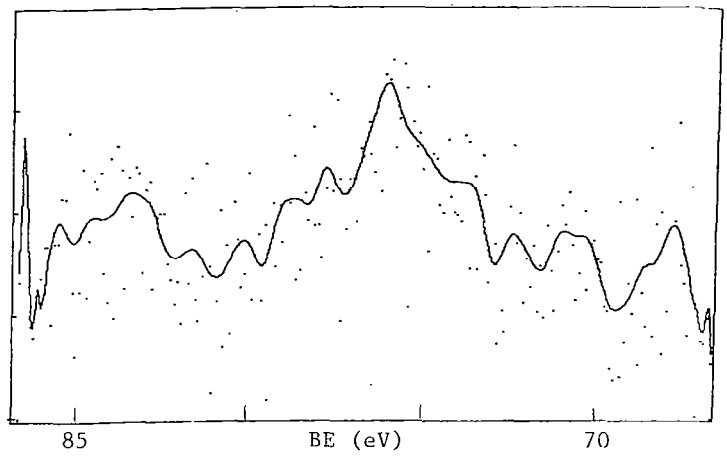

Fig. 57. Al 2p Photopeak - NASA 75-A-161 - Raw Data

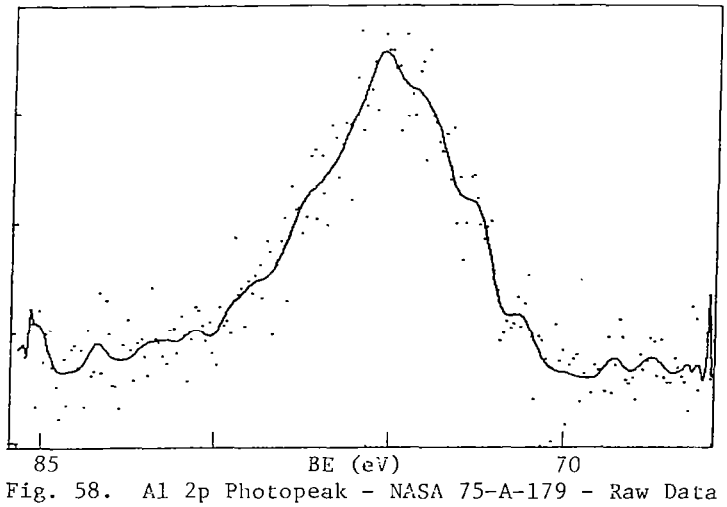

Fig. 58. Al 2p Photopeak - NASA 75-A-179 - Raw Data

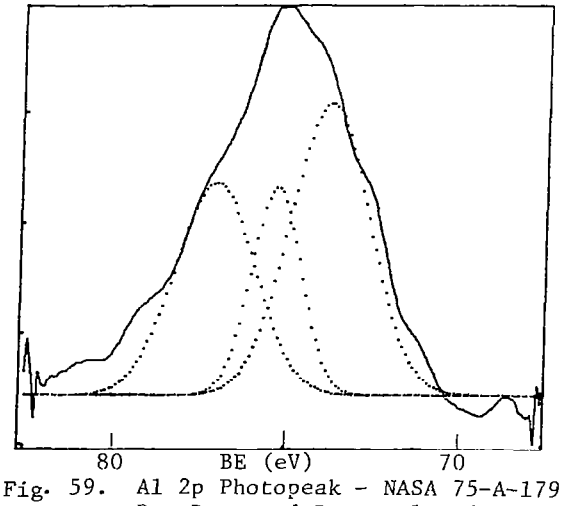

Fig. 59. Al 2p Photopeak - NASA 75-A-179 - Raw Data and Deconvoluted Components

components. Only three components were selected because the ESCA data on the authentic samples indicated that only three ranges of aluminum 2p binding energies were noted. Furthermore, it was reasoned that a prediction of more than three components in the NASA filter spectra would unnecessarily complicate the interpretation of the results. In addition, examination of the data for the standard samples does not justify consideration of more than three components.

The deconvoluted peaks shown in Figures 54 and 56 for NASA 75-A-20 and NASA 75-A-47, respectively, give binding energies for aluminum in the region of about 77.0, 75.2 and 74.0 eV (Table X). Upon comparison of these data with those for the standard samples (Table IX) it is evident that the filter samples are much like $AlCl_3$. The three Al 2p binding energies for the NASA test filters suggest that the samples are a mixture of $AlCl_3$, Al_2O_3, and $Al_2O_3.nH_2O$. In addition, it could also be argued that the lower binding energy data support the presence of aluminosilicate minerals on the filters. In the absence of supporting ancillary silicon and metal analysis, this suggestion cannot be confirmed.

Of particular significance is the fact that little or no aluminum was detected on NASA samples 75-A-161 (S204) and 75-A-174 (P4) as gauged from Figure 57. From the NAA data it could be predicted that large quantities of aluminum should be present on these filters. However, it is not surprising to find no aluminum in these filters by ESCA since the SEM photomicrographs revealed no particles on these filters. It should be pointed out that a hint of aluminum does appear in Figure 57, but the data are too noisy to confirm the presence of aluminum much less determine the species present.

The background samples (75-A-179, 181) also showed aluminum 2p photopeaks as seen in Figure 58, that are similar in appearance to those for the test filters. It is significant to point out that the background samples were collected for a 24 hour period while the flight test samples were collected during a much shorter time period. Interpretation of the ESCA data for the background samples indicates that similar aluminum-containing species are present here. This may be reasonable since the source of the background aluminum could be due to aluminum from minerals, other sources, and/or rocket exhaust particulate matter.

The most significant aspects of the study of the KSC samples are twofold. The SEM photomicrographs clearly distinguish between rocket launch collected samples and background samples. The launch particulate matter is characterized by spherical aluminum-containing particulates. The background sample particulate matter is varied in size and shape. Secondly, the ESCA measurements indicate that aluminum-containing particles were collected and their chemistry elucidated. It was found that at least three chemically different aluminum species were collected in the rocket exhaust cloud, namely, $AlCl_3$, Al_2O_3, and $Al_2O_3.nH_2O$.

3. Quantitative aspects of aluminum ESCA data: Comparison with SEM and NAA.

In Table XI are collected data on representative ESCA measurements for aluminum on Nuclepore filters. The table contains the quantity of aluminum as determined by NAA. In addition, the pertinent ESCA measurement parameters and conditions are included. It will be noted that between 178 and 76 scans were carried out in order to detect aluminum. The number of hours of scanning varied from sample to sample and thus

TABLE XI

DETAILED QUANTITATIVE ESCA ANALYSIS

OF NASA-KSC SAMPLES

	75-A-20 P4	75-A-21 P-2	75-A-41 A-1	75-A-47 A-7	75-A-161 S204	75-A-174 P4	75-A-179	75-A-181
NAA (μgm, Al)	1.84	1.34	16	4.7	2.03	7.68	2.47	2.74
Net wt. particles (μgm)	181	137	406	141	-	0	450	357
Total Run Time (hrs.)	39.5	20	21	19	20	23	24.5	22.9
Total Run Time Al (hrs.)	30.0	15	15.8	12.6	13.5	17.2	18.3	17.2
Net Al cts.	2310	2998	2978	1897	644	571	1637	1335
No. Scans	178	90	95	76	81	103	110	103
Cts. (Al)/scan	13.0	33.3	31.3	25.0	8.0	5.5	15.9	13.0
Net Si cts.	5342	2156	5918	1350	3237	3924	742	2266
Cts. (Si)/scan	30.0	24.0	62.3	17.8	39.9	38.1	6.7	2.20
Al/Si (cts./scan ratio)	0.43	1.4	0.50	1.4	0.20	0.15	2.20	5.9
SEM Photo: Particle total area μm^2	many part	many part	38	201	No unique particles	No unique particles	Many mixed particles	Many mixed particles

the net number of counts also varied. An important parameter for aluminum is the number of counts per scan. This number is calculated from the net number of counts and the number of scans. Only the net number of counts was used rather than an integral number of counts, since the Al 2p peaks were of approximately the same shape and width. These calculated counts per scan are related to the total aluminum in the sample as detected by ESCA. The smallest number of counts/scan was obtained for NASA filters 75-A-161 (S204), and 75-A-174 (P4) and in fact this ratio is probably a lower limit that indicates no aluminum present. Examination of Figure 40 reveals that the count difference for the filters is largely due to scatter and noise in the counting statistics and not due to aluminum. For the other samples in which aluminum was detected, the counts/scan ratio varies from 13 to 33. The results for 75-A-20 and 75-A-21 indicate that for #20 the longest scan time was required (30 hrs.) to obtain a reasonable Al signal of 13 counts/scan. Similarly for the aircraft samples 75-A-41 and 75-A-47 the Al values are 31.3 and 25.0 counts/scan, respectively. The aluminum content on the background samples is somewhat (approximately half) less than that for the aircraft samples. This is as expected since the exhaust cloud apparently contains only spherical aluminum-containing particles.

In order to explore the possible quantitative aspects of the ESCA data, the Al 2p count is tabulated relative to the corresponding Si 2p or 2s data. This ratio should in effect normalize the count data since the silicon in the filter should represent a constant background or reference level. This assumes that the particles themselves do not contain a significant amount of silicon. This assumption seems valid

because the number of particles and the area covered by the particles is small compared to the area of the filter exposed. The important Al/Si count ratios are for NASA samples 75-A-20, 75-A-21, and 75-A-41 and 75-A-47. For #20 the ratio is 0.43 and for #21 the ratio is 1.4. A comparison of the SEM photomicrograph for these two filters (Figure 34 and 35) reveals that filter 21 contains the greatest number of particles. It should be noted that the SEM photomicrographs shown in Figures 34-41 are representative of the whole filter and are not unique to the area sampled. This observation is directly comparable to the ESCA Al/Si ratio 1.4 to 0.43, which indicates a greater quantity of aluminum on filter 75-A-21. A clearer test of this treatment can be carried out for filters 75-A-41 and 75-A-47 which contain a fewer number of particles. The Al/Si ratios are 0.50 and 1.40, respectively. From an examination of the total particle area present, the values are $38\mu m^2$ (75-A-41) and $201\mu m^2$ (75-A-47). This ratio (ie.(201/38))=5.3 is approximately equal to the ratio of the Al/Si count ratio (ie.(1.4/0.5))=2.8 for filters 75-A-41 and 75-A-47. The near equality of these ratios is rather good when account is taken of the crude approximation used to obtain the values. It should be recognized that this result is not in agreement with the NAA data. Since no limits of accuracy have been placed on the NAA results, it is not possible at this time to comment on the discrepancy between the NAA results and the ESCA-SEM treatment of the data. It is particularly noteworthy that the ESCA-SEM treatment of the data is most successful for filters 75-A-41 and 75-A-47. This is no doubt due to the fact that these samples contain particles solely from the rocket exhaust cloud and do not

contain particulate matter from ground debris or other sources. Nevertheless, these results and the treatment of the data point out and strongly emphasize the fact the ESCA results may in some instances be of value in quantitative analysis.

V. SUMMARY AND CONCLUSIONS

Samples of airborne particulate matter collected on gold-coated and uncoated Nuclepore filters at Norfolk, Virginia and at the NASA-Kennedy Space Center (KSC) were analyzed by neutron activation analysis (NAA), by scanning electron microscopy (SEM), and by electron spectroscopy for chemical analysis (ESCA).

For the Norfolk samples, the SEM photomicrographs showed a high density of particles having a broad size distribution. Calcium, aluminum (silicon), sodium, chlorine, potassium, and magnesium were the most abundant elements detected by NAA with smaller amounts of titanium, zinc and cadmium.

A complete listing of the ESCA results for the Norfolk samples is contained in Tables IV-V. Calcium, silicon, sulfur, nitrogen, chlorine, mercury and sodium were detected by ESCA. Potassium, magnesium, and cadmium were not detected by ESCA. All samples contained silicon since it is present as a surface coating on Nuclepore filters. It was not possible to differentiate between silicon in the filter and silicon collected as particulate matter. Calcium was present as Ca^{2+} while sodium and chlorine were present as Na^{+} and Cl^{-}. In several samples, evidence was obtained for the presence of elemental mercury presumably due to contamination. Sulfur 2p photopeaks characteristic of sulfide, SO_2, sulfite, sulfate and thiosulfate species were detected. Nitrogen 1s photopeaks of ammonia (or amines), amides (or higher oxidation states such as N_2O, NO) and cyano-containing materials were noted.

For the NASA-KSC samples, the SEM photomicrographs showed particulate matter on all filter samples except those used for collection at ground stations during an aborted launch activity. The photomicrographs showed a low density of particles having a narrow size distribution. The shape and size of the particles collected at launch on ocean vessels and in airborne stations were similar. The features of the background SEM photomicrographs were similar to the Norfolk samples. Only a few particles had characteristics similar to those collected during launch activities. Aluminum was detected in all samples by NAA and the level of aluminum varied from sample to sample. The quantity of aluminum in all samples varied roughly in the order aircraft > ground station > background > ocean vessel.

A complete listing of the ESCA results for the NASA-KSC samples is contained in Tables X-XI. The aluminum detected by ESCA is due principally to $AlCl_3$, Al_2O_3, and $Al_2O_3.nH_2O$ species. This assignment is based on a comparison of measured aluminum 2p binding energies for standard aluminum-containing compounds with the binding energies for the test filters.

The following conclusions result from this ESCA study of atmospheric particles:

1. The ESCA technique cannot only detect and identify, but can establish the valence state of elements in particles ($\simeq$ 2.5μm diameter) collected at low densities on Nuclepore filters.

2. No special pretreatment of Nuclepore filters such as gold coating is necessary for ESCA analysis.

3. The $2p_{1/2,3/2}$ level of silicon contained in Nuclepore filters can be used as a convenient internal standard for measuring absolute binding energies.

4. Particular attention is called to the fact that the valence states of nitrogen and sulfur were readily determined by ESCA. Further, aluminum and silicon could be readily differentiated using ESCA.

The cooperation of Frank Mitsianis during the scanning electron microscopy study is greatly appreciated. Thanks to Andy Mollick of the Glassblowing Shop for his assistance in constructing the apparatus to collect the authentic dust samples. A note of thanks is also extended to Mitch Koppelman for his aid in the deconvolution of the ESCA spectra. This work was supported under NASA Contract NAS1-13175-2 including a graduate research assistantship for one of us (RDS). The technical assistance of K. H. Crumbly, R. W. Storey, Jr. and D. C. Woods of the NASA-Langley Research Center was appreciated.

VI. REFERENCES

1. R. W. Storey, Jr. et al., NASA Report TMX-3785, Washington, D.C., December, 1975.

2. R. J. Bendura and K. H. Crumbly, NASA Report TMX-3539, Washington, D.C., Sept., 1977.

3. Remote Measurement of Pollution. NASA Special Publication 285, 1971.

4. Study of Man's Impact on Climate. Inadvertent Climate Modification. M.I.T. Press, 1971.

5. Study of Critical Environmental Problems. Man's Impact on the Global Environment. M.I.T. Press, 1970.

6. F. S. Harris, Jr., NASA Report CR-2626, Washington, D.C., Jan., 1976.

7. K. Siegbahn, C. Nordling, A. Fahlman, R. Nordberg, K. Hamrin, J. Hedman, G. Johansson, T. Bergmark, S. Karlsson, I. Lindgren, and B. Lindberg, "Electron Spectroscopy for chemical Analysis: Atomic, Molecular, and Solid State Structure Studies by Means of Electron Spectroscopy," Almqvist and Wiksell, Stockholm, Sweden, 1967.

8. L. D. Hulett, T. A. Carlson, B. R. Fish, and J. L. Durham, Determination of Air Quality, Symposium Procd. 161st National ACS Meeting, 1971, Plenum Press, New York, N.Y., p. 179.

9. T. Novakov, P. K. Mueller, A. E. Alcocer, and J. W. Otvos, J. Colloid and Interface Sci., 39, 225 (1972).

10. N. L. Craig, A. B. Harker, and T. Novakov, Atmos. Environ., 8, 15 (1974).

11. Y. E. Arakting, N. S. Bhacca, W. G. Proctor, and J. W. Robinson, Spectrosc. Lett., 4, 365 (1971).

12. D. N. Hendrickson, J. M. Hollander, and W. L. Jolly, Inorg. Chem., 8, 2642 (1969).

13. G. R. Grieger, Am. Lab., 77 (1976).

14. S. G. Chang and T. Novakov, Atmos. Environ., 9, 495 (1975).

15. J. J. Jack and D. M. Hercules, Anal. Chem., 43, 729 (1971).

16. R. Nordberg, H. Brecht, R. G. Aldridge, A. Fahlman, and J. R. VanWazer, Inorg. Chem., 9, 2469 (1970).

17. H. D. Schultz, C. J. Vesely, and D. W. Langer, Applied Spectrosc., 28, 374 (1974).

18. D. S. Urch and S. Murphy, J. Electron Spectrosc. Relat. Phenom., 5, 167 (1974).

19. P. R. Anderson and W. E. Swartz, Inorg. Chem., 13, 2293 (1974).

20. J. R. Lindsay, H. J. Rose, W. E. Swartz, P. H. Watts, and K. R. Rayburn, Applied Spectrosc., 27, 1 (1973).

21. I. Adams, J. M. Thomas, and G. M. Bancroft, Earth Planet. Sci. Lett., 16, 249 (1972).

22. W. T. Huntress and L. Wilson, Earth Planet. Sci. Lett., 15, 59 (1972).

23. C. R. Cothern, D. W. Langer, and C. J. Vesely, J. Electron Spectrosc. Relat. Phenom., 3, 399 (1974).

24. D. C. Frost, W. R. Leeder, and R. L. Tapping, Fuel, Lond., 53, 206 (1974).

25. R. D. Seals, R. Alexander, L. T. Taylor, and J. G. Dillard, Inorg. Chem., 12, 2485 (1973).

26. G. W. Dulaney, GASCAP IV, VPI&SU, 1969, (G.W.D., now at Digital Equipment Corp., Maynard, MA).

27. D. J. Fabian, J. Fuggle, L. M. Watson, A. Barrie and D. Latham, "X-Ray Photoelectron Studies of Aluminum and Aluminum-Gold Alloys," in Bond Structure Spectroscopy of Metals and Alloys, ed. D. J. Fabian, and L. M. Watson, Academic Press Inc., New York, NY., 1973, p. 91.

28. D. E. Brownlee, G. V. Ferry and D. Tomandl, Science, 191, 1270 (1976).

29. R. R. Bailey and J. P. Wightman, NASA Report CR-2929, Washington, D.C., February, 1978.